

# Estimation of temperature-dependent growth profiles for the assessment of time of hatching in forensic entomology

D. Pigoli<sup>1</sup>, J.A.D. Aston<sup>2</sup>, F. Ferraty<sup>3</sup>, A. Mazumder<sup>4</sup>, C. Richards<sup>5</sup>, and M.J.R. Hall<sup>6</sup>

<sup>1</sup>Department of Mathematics, King's College London

<sup>2</sup>Statistical Laboratory, DPMMS, University of Cambridge

<sup>3</sup>Toulouse Mathematics Institute, University of Toulouse

<sup>4</sup>Department of Statistics, Carnegie Mellon University

<sup>5</sup>Agriprotein Technologies

<sup>6</sup>Department of Life Sciences, Natural History Museum, United Kingdom

## Abstract

Forensic entomology contributes important information to crime scene investigations. In this paper, we propose a method to estimate the hatching time of larvae (or maggots) based on their lengths, the temperature profile at the crime scene and experimental data on larval development. This requires the estimation of a time-dependent growth curve from experiments where larvae have been exposed to a relatively small number of constant temperature profiles. Since the temperature influences the developmental speed, a crucial step is the time alignment of the curves at different temperatures. We propose a model for time varying temperature profiles based on the local growth rate estimated from the experimental data. This allows us to estimate the most likely hatching time for a sample of larvae from the crime scene. Asymptotic properties are provided for the estimators of the growth curves and the hatching time. We explore via simulations the robustness of the method to errors in the estimated temperature profile. We also apply the methodology to data from two criminal cases from the United Kingdom.

## 1 Introduction

In cases of suspicious death, forensic entomologists can provide reliable information about the minimum post mortem interval from the blowfly larvae collected from the body at the scene. This evidence depends on the fact that blowfly development is predictable and depends on the temperature. However, while experimental data are usually collected at constant temperatures, real life scenes are subjected to dynamic temperature profiles. In this work, we apply techniques from functional data analysis (FDA; Ramsay and Silverman, 2005; Ferraty and Vieu, 2006; Horváth and Kokoszka, 2012) to reconstruct the growth curve of the larvae in the presence of a varying temperature profile, using information from experiments run at constant temperature. The objective is the assessment of the time since colonization, which is the interval between the earliest time when the observed blowflies laid their eggs and the time when samples are collected at the scene. The current approach is to use a linear accumulated degree hours model (see below) which uses an average temperature approach. A more accurate assessment of the hatching time for a given set of larvae, via an case specific growth curve, would be a useful addition to the forensic science toolbox.

From the statistical perspective, FDA is the field that investigates the statistical properties of curves and surfaces. It has also started to be of interest in forensic entomology, with one preliminary investigation using the technique for thermal wavelength analysis of maggot populations for time of death prediction (Warren et al., 2017). Here, we use the well known connections of FDA to growth curve analysis (Ramsay and Silverman, 2005). The main challenge in this paper is the need to combine different sources of information about the growth process to estimate the most likely growth curve that led to the larval lengths observed at the scene. Larval developmental data are collected in incubators which keep the temperature constant, while larvae at the crime scene are exposed to a varying temperature profile. The first part of the methodology requires an estimate of the actual case specific growth curve from the growth curves observed at constant temperatures in the lab. Then, the hatching time that leads to the best fit of the measured larval lengths at the crime scene is selected. We provide asymptotic results both for the estimator of the growth curve and of the hatching time and we assess the finite sample properties of the procedure via simulation studies. Finally, we discuss the application of the method to the data from two investigations in the United Kingdom.

## 1.1 Forensic Entomology

Forensic entomology is the study of insects (and other arthropods) in relation to criminal investigation, frequently involving insect evidence in cases of suspicious death. A great diversity of insects are attracted to decomposing human corpses, both to feed and to lay their eggs or larvae. Flies and beetles are the most common visitors, as both immature insects (larvae or maggots) and adults. In particular, blowflies are among the most important insects in criminal investigation, because they are usually the first to arrive (Greenberg, 1991). While the methods described in this work could be applied in general to any insects of forensic interest, we will consider here two species of blowfly, *Calliphora vicina* and *Calliphora vomitoria*.

Fly larvae are usually used to estimate a lower bound for the time since death. Indeed, the age of the oldest insects on the body provides an assessment of when the mother insects gained access to the body and, as a consequence, a lower bound for the post-mortem interval in a criminal investigation. In this work we focus in particular on the information that is possible to obtain from the length of the larvae observed on the body or at the crime scene. The life cycle of flies is divided into different stages. In the case of an outdoor crime scene, adult female blowflies can arrive within just a few hours to lay eggs on the body (Reibe and Madea, 2010). The eggs then hatch into first instar larvae (commonly called maggots) which start feeding and develop into second and then third instar larvae (between these stages, the cuticle is shed to allow for growth). When larvae have finished feeding, they move away from the body and metamorphose into immobile puparia within which the pupal and pharate adult stages develop (Martín-Vega et al., 2017). Finally, adult flies emerge from puparia and begin a new cycle.

The rate of development of fly larvae is temperature dependent and when comparing the specimen observed at the crime scene with experimental data it is essential to adjust with respect to the different temperatures. Currently, the standard technique used to estimate the rate of development with temperature compensation is the Accumulated Degrees Hours (ADH) model. This consists in summing the hours of development multiplied by the temperature (in C), thus providing a rough measure of the amount of thermal energy available to the larva. This can then be compared with existing experimental results about how many ADH are needed to reach each developmental stage in the insect life cycle and from this deduce the time of colonization at the scene (Amendt et al., 2007). Our goal is to explore how to provide more refined methods that look into the growth dynamic between hatching and pupation. We will rely on experimental developmental data on larval lengths for *Calliphora vicina* and *Calliphora vomitoria* (Richards

et al., 2017) to achieve this.

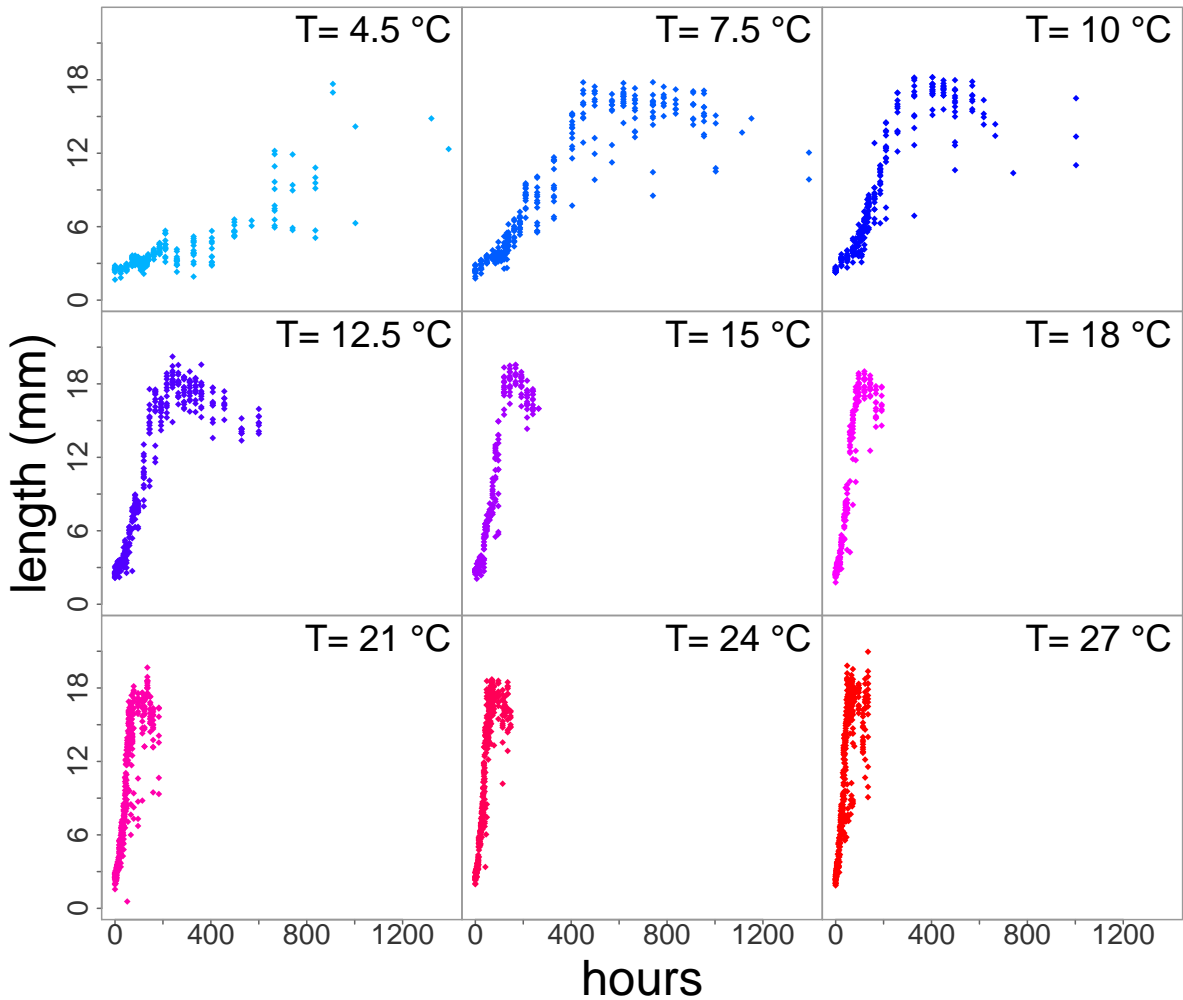


Figure 1: Experimental developmental data for *Calliphora vicina*, measured at 9 different constant temperature profiles.

## 2 Model and methods

The fact that larval development depends mainly on temperature is well known in forensic entomology (Amendt et al., 2007; Donovan et al., 2006). However, laboratory experiments are bound to measure this relationship only for a relatively small numbers of simple (usually constant) temperature profiles. Our first goal is to use techniques from functional data analysis and nonparametric regression to estimate the expected growth curve corresponding to more realistic temperature profiles. Once the growth lengths are available for any temperature profile, one is able to estimate the hatching time and hence the post mortem interval from data available at the scene.

## 2.1 Estimation of the growth process

In a typical larval developmental data set, we have  $K$  experimental temperatures  $T_1 < T_2 < \dots < T_K$  and, for each species of interest, one observes the larval lengths  $Y_{kjl}$  measured at time  $t_j^k$  after hatching,  $t_1^k, \dots, t_{n_k}^k$ , for  $l = 1, \dots, N_{kj}$  individual larvae which has been exposed to a constant experimental temperature  $T_k$ ,  $k = 1, \dots, K$ . The observation times  $t_1^k, \dots, t_{n_k}^k$  may differ across experimental temperatures, generally being set at greater intervals for lower temperatures. Figure 1 displays an example of this kind of experimental data for *Calliphora vicina*. In these data, the hatching time  $t_h$  is systematically set to zero (i.e.  $t_h = t_1 = 0$ ) so that it is the time reference.

We can then assume that the observed lengths satisfied a non-parametric regression model

$$Y_{kjl} = L_{T_k}(t_j) + \epsilon_{kjl},$$

where  $\epsilon_{kjl}$  are independent, zero mean random variables and the mean larval length curve  $L_{T_k}(t)$  depends on the experimental temperatures  $T_k$ ,  $k = 1, \dots, K$ . It is then possible to estimate  $L_{T_k}(t)$  by means of a nonparametric smoothing estimator. In this work, we use a local linear regression estimator, but others could also be used if preferred. The local linear regression provides estimates  $\hat{L}_{T_k}(t)$  for all the constant temperature growth curves. Figure 2 displays the estimated growth curves  $\hat{L}_{T_1}(t), \dots, \hat{L}_{T_K}(t)$  at any time  $t$  in their respective time ranges for the *Calliphora vicina* data.

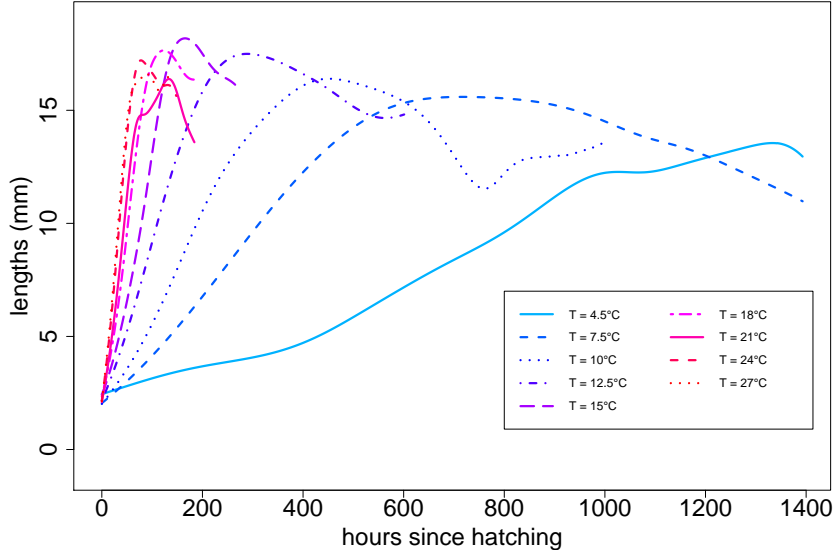


Figure 2: Smooth experimental growth curves estimated from the *Calliphora vicina* lengths measured at constant temperature  $T$ .

The question now is how to produce an estimate for the growth curve at a grid of time points  $t_1, \dots, t_p$  associated to a generic temperature profile  $T(t_1), \dots, T(t_p)$ . We claim that, if we consider a small enough time interval, the temperature in that interval can be considered roughly constant and therefore the growth process would be bound to follow the local dynamics of the correspondent constant temperature growth curve *at the corresponding stage of the growth process*, i.e. at the point of the curve which reaches the current length in the growth process. This suggests the following model for the local growth process:

$$\frac{d L(t)}{dt} \Big|_{t=t_k} = \frac{d L_{T(t_k)}(u)}{du} \Big|_{u=(L_{T(t_k)})^{-1}(L(t_k))}, \quad (1)$$

where  $L_{T(t_k)}$  is the growth profile at constant temperature  $T(t_k)$  and  $L(t)$  is the growth profile with varying temperature. The differential equation model (1) can be reformulated as  $L'(t) = L'_{T(t_k)} \circ L_{T(t_k)}^{-1} \circ L(t_k)$  where  $L'$  stands for the derivative of  $L$  and the symbol  $\circ$  refers to the usual composition operator between real-valued functions. This dynamic model means that the (expected) local increment in length at time  $t_k$  is the one that would occur in the growth profile at constant temperature  $T(t_k)$  when the length is equal to  $L(t_k)$ . This allows to reconstruct the varying temperature growth profile iteratively, as a discretised solution to the above ODE:

$$\begin{cases} L(t_1) = L_{T(t_1)}(t_1) \\ L(t_{k+1}) = L(t_k) + (t_{k+1} - t_k) \left\{ L'_{T(t_k)} \circ L_{T(t_k)}^{-1} \circ L(t_k) \right\}, \quad \text{for } k = 1, \dots, p-1, \end{cases}$$

with  $T(t_1), \dots, T(t_p)$  being the varying temperature profile.

This would solve the problem if we knew the expected growth curve  $L_T$  for any temperature  $T$  we can observe, but in practice we can have experimental data only for a relatively small set of temperatures. We need therefore to estimate first the growth profile  $L_T$  for a generic temperature  $T$  from a set of estimated growth curves  $\tilde{L}_{T_1}, \dots, \tilde{L}_{T_K}$ . The main difficulty here is that the temperature influences the speed of the growth process. Using the language of FDA, these curves present both amplitude and phase variation (see Ramsay and Silverman, 2005; Marron et al., 2014), as can be appreciated from the example of the *Calliphora vicina* experimental data and their estimated constant temperature growth curves in Figure 2.

At this stage, one postulates that the experimental growth curves  $\tilde{L}_{T_1}(t), \dots, \tilde{L}_{T_K}(t)$  have corresponding profiles in a standardized time scale  $\tilde{S}_{T_1}, \dots, \tilde{S}_{T_K}$ . These can be obtained using warping transformations  $\tilde{w}_{T_1}, \dots, \tilde{w}_{T_K}$ , acting over the time in such a way, for any  $k = 1, \dots, K$ ,  $\tilde{S}_{T_k} \circ \tilde{w}_{T_k}(t) = \tilde{L}_{T_k}(t)$ . The warping functions can be determined via a landmark registration procedure that aligns hatching time, time of maximum length and pupation time of the growth processes. It is of course possible to resort to more advanced registration methods but the relatively simple shape of the growth curves allows landmark registration to perform well, as it can be seen for the example of *Calliphora vicina* growth curves, whose registered growth curves and warping functions can be found in Figure 3.

From the registration procedure, one has at hand  $K$  estimated growth shapes  $\tilde{S}_{T_1}, \dots, \tilde{S}_{T_K}$  and estimated warping functions  $\tilde{w}_{T_1}, \dots, \tilde{w}_{T_K}$ . These are now defined on the same domain and this allows us to estimate across temperatures to predict the growth process for any constant temperature  $T$ .

For any  $T$ , we reconstruct the growth shape and warping function by function-on-scalar non-parametric regression (see Ferraty et al. 2011) as

$$\hat{S}_T(u) = \frac{\sum_{k=1}^K \tilde{S}_{T_k} K_S(h_S^{-1}(T_k - T))}{\sum_{k=1}^K K_S(h_S^{-1}(T_k - T))} \quad (2)$$

and

$$\hat{w}_T(t) = \frac{\sum_{k=1}^K \tilde{w}_{T_k} K_w(h_w^{-1}(T_k - T))}{\sum_{k=1}^K K_w(h_w^{-1}(T_k - T))}, \quad (3)$$

where  $K_S$  and  $K_w$  are kernel functions and  $h_S$  and  $h_w$  suitably chosen bandwidth.

Finally, the estimated growth process at constant temperature  $T$  will be  $\hat{L}_T(t) = \hat{S}_T \circ \hat{w}_T(t)$ . These curves can be used to reconstruct the growth curve for any temperature profile. However, a few technical issues need to be considered. First, as the growth curve is not monotone, there

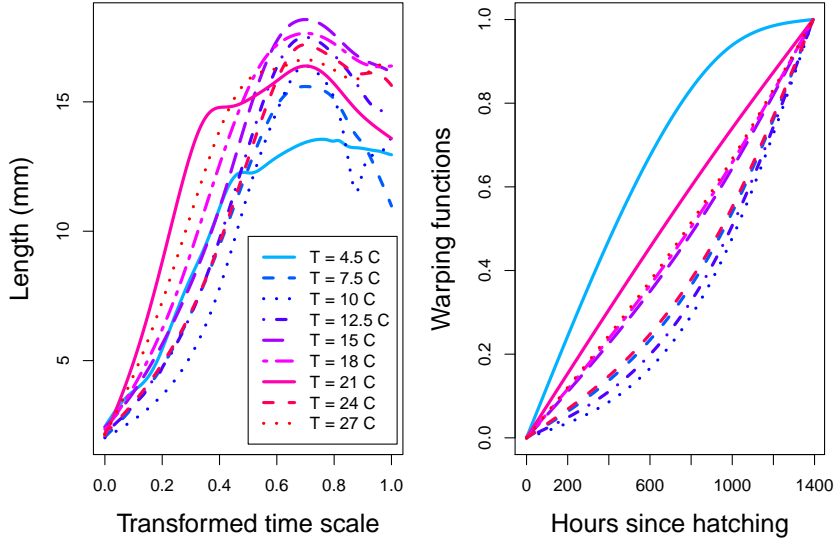


Figure 3: Experimental growth shapes.

may be multiple times  $t$  at which  $L_{T(t_k)}(t) = L(t_k)$ . In particular, we need to distinguish between the feeding phase (initial monotone increase in length up to the maximum) and the post-feeding phase (the usually decreasing region after the maximum). To do this, as long as  $\max_{l \leq k} L(t_l) < \max_t L_{T(t_k)}(t)$  the process is labelled as increasing and the positive value of  $L'_{T(t_k)} \circ L_{T(t_k)}^{-1} \circ L(t_k)$  is used to obtain the length at  $t_{k+1}$ . Otherwise, the process is considered as post-feeding and the point corresponding to the negative derivative is used to update the length. Moreover, once the process is in the post-feeding phase, if the length reaches the minimum post-maximum value for the current temperature, i.e. if  $L(t_k) \leq \hat{S}_{T(t_k)}(1)$ , we assume that the process gets to pupation and the larval length is not defined from that time on.

## 2.2 Estimation of the hatching time

We now want to use the estimated temperature-dependent growth profile to select the most likely hatching date given a set of length measurements taken at a time  $t^*$  where the reference time is the local one. To do that, we are going to compare the growth profiles that would be expected if the hatching time  $t_h$  was at any time between the last time the victim has been seen alive  $t_a$  and  $t^*$ . Let  $L(t - t_h)$ ,  $t_h \leq t \leq t^*$ , be the growth curve for hatching time equal to  $t_h$  and temperature profile  $\{T(t^* - t); t_h \leq t \leq t^*\}$ . Let then  $Y_i^*, i = 1, \dots, n_{obs}$  be the measured larval lengths

$$Y_i^* = L(t^* - t_h) + \epsilon_i, \quad (4)$$

with  $\epsilon_i, i = 1, \dots, n_{obs}$  independent random errors with zero mean and unknown variance  $\sigma^2$ . Then, we can estimate  $t_h$  as

$$\hat{t}_h = \arg \min_{t_a \leq t \leq t^*} \sum_{i=1}^{n_{obs}} \left( \hat{L}(t^* - t) - Y_i \right)^2 = \arg \min_{t_a \leq t \leq t^*} \left( \hat{L}(t^* - t) - \bar{Y} \right)^2, \quad (5)$$

i.e. we choose the hatching time whose expected length at time  $t^*$  best fits the observed values. However, we may also want to include some expert knowledge in the estimation procedure. First, the forensic entomologist collecting the sample may recognise that the larvae reached (or

not) the post-feeding phase, i.e. the region of the growth curve after the peak where larvae stop feeding in preparation of pupation and therefore they decrease in length. We can easily integrate this piece of information in the estimation procedure by restricting the admissible region for the minimisation problem (5) to the hatching times whose associated growth process at time  $t^*$  has already reached (or not) the postfeeding region, i.e. the estimated derivative is negative at some time  $t \leq t^*$ . If we are willing to assume a parametric model for the error, we can also build an approximate confidence interval for the hatching time, for example by inverting the region of non rejection of the likelihood ratio test, i.e. the confidence region will be  $CR(\alpha) = \{t : l(t) > l(\hat{t}_h) - \chi^2_{1-\alpha}(1)/2\}$ , where  $l$  denotes the log-likelihood and  $\chi^2_{1-\alpha}(1)$  the  $1 - \alpha$  quantile of the  $\chi^2$  distribution with 1 degree of freedom. However, this region is not necessary convex and we may prefer a more conservative interval defined as  $CI(\alpha) = [\min CR(\alpha), \max CR(\alpha)]$ . This is a connected interval that, by construction, asymptotically guarantees at least a  $(1 - \alpha)\%$  coverage of the hatching time. To be coherent with the estimation procedure above, we also need to account for the information about the developmental stage of the observed larvae. Since we optimised the criterion only in the admissible region of hatching time which guarantees the correct developmental stage (postfeeding or not) at the time of sample collection, we need to do the same for the parameter space where the log-likelihood is defined. This is then restricted to the same set of hatching times used in the estimation.

On the other hand, one may want to include prior information about the hatching time, coming for example from the investigative activity (in addition to the interval of admissible hatching times). Let us assume we can translate this information into a prior distribution on the parameter  $t_h$ , so that  $t_h \sim \pi$  where  $\pi$  is a known distribution. We can then use Bayes theorem to update the information about  $t_h$  given the observed larval lengths and derive a posterior distribution for  $t_h$ . For example, assuming a normal distribution for the errors we have

$$f(t_h|Y_i) \propto \exp \left( - \sum_{i=1}^{n_{obs}} \frac{\{Y_i - L(t^* - t_h)\}^2}{2\sigma^2} \right) \pi(N^*). \quad (6)$$

In practice we need to substitute  $\sigma^2$  with a plug-in estimate, for example the sample variance of the observed lengths and  $L(t^* - t_h)$  with the estimated quantity  $\hat{L}(t^* - t_h)$ . Note that in the estimation procedure in this section, we are ignoring the uncertainty in the estimation of the time-dependent growth process. This is indeed present and, while the uncertainty from the experimental data is usually negligible, errors on the temperature at the crime scene can affect the results. We are going to explore this issue through simulation studies in Section 4.1. Note that it is straightforward to generalise these ideas to the case where more than one species of larvae (for which developmental data are available) are observed. Let  $Y_{ij}^*$  be the observed length of the  $i$ -th sample from the  $j$ -th species,  $j = 1, \dots, J$ ,

$$Y_{ij}^* = L^{(j)}(t^* - t_h) + \epsilon_{ij},$$

with  $\epsilon_{ij}$ ,  $i = 1, \dots, n_j$  independent random errors with zero mean and unknown variance  $\sigma_j^2$ . Then,

$$\hat{t}_h = \arg \min_{t_a \leq t \leq t^*} \sum_{j=1}^J \frac{\sum_{i=1}^{n_j} \left( \hat{L}^{(j)}(t^* - t) - Y_{ij}^* \right)^2}{\hat{\sigma}_j^2/n_j}, \quad (7)$$

where  $\hat{\sigma}_j^2$  is the sample variance of the lengths of the  $j$ -th species.

### 3 Asymptotic properties

The main goal of this section is to state the asymptotic properties of the estimated hatching time, giving theoretical justification for our estimators, in addition to the empirical justification

that we will gain in the next section. To this end, the estimating procedure is decomposed into four steps. In the first step the constant temperature growth profile  $L_{T_k}(\cdot)$  and its derivative  $L'_{T_k}(\cdot)$  are estimated from observed growth data set at a given ambient constant temperature  $T_k$  belonging to the fixed design  $T_1, \dots, T_K$ . A decomposition of the estimated constant temperature growth profile  $L_{T_k}(\cdot)$  into rescaled growth shape  $S_{T_k}(\cdot)$  and warping function  $w_{T_k}(\cdot)$  is achieved in step 2, at a given ambient temperature  $T_k$  taken in the same fixed design. Step 3 focuses on the estimation of the constant temperature growth-profiles  $L_T(\cdot)$  and its derivative  $L'_T(\cdot)$  at any ambient temperature  $T$  (i.e.  $T$  may be outside the fixed design  $T_1, \dots, T_K$ ). In the last step the asymptotic behaviour of the estimated hatching date  $\hat{t}_h$  is provided. All proofs and assumptions are postponed to the appendices. In order to make the theoretical developments more readable and accessible, the framework is voluntarily restricted to fixed designs, non random temperatures and only one species of fly. However, the setting can, of course, be extended to random designs, random temperatures and several species of fly, subject to some straightforward adjustments

*Step 1: Estimating constant temperature growth profiles.*

For a given constant temperature  $T_k \in \{T_1, T_2, \dots, T_K\}$  one observes repeated larvae growth lengths  $\{Y_{kjl}; j = 1, \dots, n_k, l = 1, \dots, N_{kj}\}$  at a grid of  $n_k$  time after hatching  $0 = t_1^k < t_2^k < \dots < t_{n_k}^k := t_{pup}^k$ . From this sample, one derives the benchmark growth profile  $L_{T_k}(t)$  at constant temperature  $T_k$  and time after hatching  $t$  by means of the nonparametric regression model

$$Y_{kjl} = L_{T_k}(t_j) + \varepsilon_{kjl},$$

and the local linear regression estimator (see for instance Fan 1992, Fan and Gijbels 1992, Fan 1993, and Ruppert and Wand 1994):

$$(\hat{a}, \hat{b}) = \arg \min_{a, b} \sum_{j=1}^{n_k} \omega_k(t_j^k) \left\{ \bar{Y}_{kj} - a - b(t_j^k - t) \right\}^2 K \left\{ h_L^{-1}(t_j^k - t) \right\},$$

with

$$\tilde{L}_{T_k}(t) = \hat{a} = (1, 0)^T (\mathbf{X}_t^T \mathbf{K}_t \mathbf{X}_t)^{-1} \mathbf{X}_t^T \mathbf{K}_t \bar{\mathbf{Y}}^k,$$

where, for any  $k$ ,  $\bar{Y}_{kj} := \frac{1}{N_{kj}} \sum_{l=1}^{N_{kj}} Y_{kjl}$ ,  $\bar{\mathbf{Y}}^k := (\bar{Y}_{k1}, \dots, \bar{Y}_{kn_k})^T \in \mathbb{R}^{n_k}$ , the  $(n_k \times 2)$  matrix  $\mathbf{X}_t = \begin{pmatrix} 1 & 1 & \dots & 1 \\ t_1^k - t & t_2^k - t & \dots & t_{n_k}^k - t \end{pmatrix}^T$ , and the  $(n_k \times n_k)$  diagonal matrix  $\mathbf{K}_t := \text{diag}(\omega_k(t_1^k) K \{h_L^{-1}(t_1^k - t)\}, \dots, \omega_k(t_{n_k}^k) K \{h_L^{-1}(t_{n_k}^k - t)\})$ . In practice, the function  $\omega_k$  is set in such a way  $\omega_k(t_j) = N_{kj}/n_k$ . The expression of the estimator of  $L'_{T_k}(t)$ , the first derivative of  $L_{T_k}(t)$ , is given by:

$$\tilde{L}'_{T_k}(t) = \hat{b} = (0, 1)^T (\mathbf{X}_t^T \mathbf{K}_t \mathbf{X}_t)^{-1} \mathbf{X}_t^T \mathbf{K}_t \bar{\mathbf{Y}}^k.$$

As it is shown in the next section, to derive the consistency for the whole estimating procedure, a uniform rate of convergence for  $\tilde{L}_{T_k}$  and its derivative  $\tilde{L}'_{T_k}$  are needed.

**THEOREM 1** *Under (H1), (H4)-(H8), for any  $T_k \in \{T_1, \dots, T_K\}$  it holds:*

$$\left\| \tilde{L}_{T_k} - L_{T_k} \right\|_\infty = O(h_L^2) + O_P \left\{ (nh_L^3)^{-1/3} \right\}, \quad (8)$$

and

$$\left\| \tilde{L}'_{T_k} - L'_{T_k} \right\|_\infty = O(h_L^2) + O_P \left\{ (nh_L^6)^{-1/3} \right\}. \quad (9)$$

Although the literature on local linear regression is dense, the proof of (8) and (9) needs some adjustments that are postponed to Appendix B.1.

*Step 2: Decomposing growth profiles into rescaled growth shape and warping functions.*

For the benchmark growth profile  $L_{T_k}(\cdot)$  at a given constant temperature  $T_k$ , one postulates the existence and uniqueness of a rescaled growth shape  $S_{T_k}$  mapping  $[0, 1]$  into  $\mathbb{R}$  and a strictly increasing warping function  $w_{T_k}$  mapping  $[0, t_{pup}^k]$  into  $[0, 1]$  such that, for any time  $t$  after hatching,  $L_{T_k}(t) = S_{T_k} \circ w_{T_k}(t)$ , where  $S_{T_k}$  and  $w_{T_k}$  are derived from  $L_{T_k}(\cdot)$  by aligning hatching time, time of maximum length  $t_{max}^k$  and pupation time  $t_{pup}^k$ . For a given real  $\alpha \in (0, 1)$  and for any  $k$  varying from 1 to  $K$ , the warping function  $w_{T_k}$  is assumed to be a quadratic polynomial such that:

$$w_{T_k}(0) = 0, \quad w_{T_k}(t_{max}^k) = \alpha, \quad w_{T_k}(t_{pup}^k) = 1.$$

In other words, the warping function  $w_{T_k}$  is a strictly increasing function interpolating the three points with coordinates  $(0; 0)$ ,  $(t_{max}^k; \alpha)$ , and  $(t_{pup}^k; 1)$ . Imposing  $w_{T_k}$  in the space of quadratic polynomials ensures uniqueness. This procedure is commonly called registration (see Ramsay and Silverman, 2005). Our aim is to state asymptotic properties of the  $K$  estimated pairs  $(\tilde{S}_{T_1}, \tilde{w}_{T_1}), \dots, (\tilde{S}_{T_K}, \tilde{w}_{T_K})$  and their corresponding derivatives  $(\tilde{S}'_{T_1}, \tilde{w}'_{T_1}), \dots, (\tilde{S}'_{T_K}, \tilde{w}'_{T_K})$ . For any  $k \in \{1, \dots, K\}$ , let  $\tilde{t}_{max}^k$  be the time of maximum length derived from the estimated growth profile  $\tilde{L}_{T_k}$ ; the estimated warping function  $\tilde{w}_{T_k}$  is defined as the strictly increasing quadratic polynomial satisfying

$$\tilde{w}_{T_k}(0) = 0, \quad \tilde{w}_{T_k}(\tilde{t}_{max}^k) = \alpha, \quad \tilde{w}_{T_k}(t_{pup}^k) = 1,$$

and the corresponding estimated rescaled growth shape  $\tilde{S}_{T_k} = \tilde{L}_{T_k} \circ \tilde{w}_{T_k}^{-1}$ , where  $\tilde{w}_{T_k}^{-1}$  is the inverse function of  $\tilde{w}_{T_k}$ .

**THEOREM 2** *Under (H1)-(H8), for any  $T_k \in \{T_1, \dots, T_K\}$ ,  $\tilde{w}_{T_k}$  (resp.  $\tilde{S}_{T_k}, \tilde{w}'_{T_k}, \tilde{S}'_{T_k}$ ) converges to  $w_{T_k}$  (resp.  $S_{T_k}, w'_{T_k}, S'_{T_k}$ ) with the same rate of convergence  $r_n = O(h_L^2) + O_P\{(nh_L^6)^{-1/3}\}$ .*

*Step 3: Estimating constant temperature growth profiles and corresponding first derivatives at any ambient temperature.*

In this step, the challenge is to estimate the constant temperature growth profile  $L_T$  at any ambient temperature  $T$  (i.e. not only in the discrete grid  $T_1, \dots, T_K$ ). Based on the  $K$ -sample  $(\tilde{S}_{T_1}, T_1), \dots, (\tilde{S}_{T_K}, T_K)$  and  $(\tilde{w}_{T_1}, T_1), \dots, (\tilde{w}_{T_K}, T_K)$  one is able to derive an estimator  $\hat{S}_T$  (resp.  $\hat{w}_T$ ) of the growth shape  $S_T$  (resp.  $w_T$ ) for any ambient temperature  $T$  (see (40) and (41)). So, for any temperature  $T$ , it is easy to deduce an estimator of the growth profile  $L_T$  by setting  $\hat{L}_T = \hat{S}_T \circ \hat{w}_T$ . Similarly, based on the  $K$ -sample  $(\tilde{S}'_{T_1}, T_1), \dots, (\tilde{S}'_{T_K}, T_K)$  and  $(\tilde{w}'_{T_1}, T_1), \dots, (\tilde{w}'_{T_K}, T_K)$ , one can derive the estimation of  $S'_T$  and  $w'_T$  at any temperature  $T$  by setting

$$\hat{S}'_T = \frac{\sum_{k=1}^K \tilde{S}'_{T_k} K_{S'} \{h_{S'}^{-1}(T_k - T)\}}{\sum_{k=1}^K K_{S'} \{h_{S'}^{-1}(T_k - T)\}} \text{ and } \hat{w}'_T = \frac{\sum_{k=1}^K \tilde{w}'_{T_k} K_{w'} \{h_{w'}^{-1}(T_k - T)\}}{\sum_{k=1}^K K_{w'} \{h_{w'}^{-1}(T_k - T)\}},$$

where  $K_{S'}$  (resp.  $K_{w'}$ ) is also a kernel function and  $h_{S'}$  (resp.  $h_{w'}$ ) the nonnegative smoothing parameter. Because  $L'_T = (S'_T \circ w_T) w'_T$ , for any temperature  $T$ , the derivative of the growth profile  $L'_T$  is estimated with  $\hat{L}'_T = (\hat{S}'_T \circ \hat{w}_T) \hat{w}'_T$ .

**THEOREM 3** *Under (H1)-(H8), for any temperature  $T$  it holds:*

$$\|\hat{L}_T - L_T\|_\infty = O(h_L^2) + O(h_S) + O_P\{(n h_L^6)^{-1/3}\}, \quad (10)$$

and

$$\left\| \widehat{L}'_T - L'_T \right\|_\infty = O(h_L^2) + O(h_{S'}) + O(h_w) + O(h_{w'}) + O_P \left\{ (nh_L^6)^{-1/3} \right\}. \quad (11)$$

*Step 4: Estimating hatching time.*

Before tackling the estimation of the unknown hatching date  $t_h$ , one focuses on the varying temperature growth length  $L(t)$  at the time  $t$  after hatching which is assumed to depend on the temperature process  $\{T(v), v \in [0, t)\}$ . One postulates that the growth length  $L(t)$  given the set of temperature variations  $\{T(v), v \in [0, t)\}$  satisfies the dynamic growth model:

$$L(t) - L(0) = \int_0^t \left( \frac{dL_{T(v)}(u)}{du} \Big|_{u=L_{T(v)}^{-1}\{L(v)\}} \right) dv = \int_0^t \left\{ L'_{T(v)} \circ L_{T(v)}^{-1} \circ L(v) \right\} dv,$$

where  $L(0) = L_{T(0)}(0)$  is the length at the hatching time. This formulation can be expressed in terms of differential equation:  $L'(t) = L'_{T(t)} \circ L_{T(t)}^{-1} \circ L(t)$ . In practice, one uses a fine grid of time  $0 = t_0 < t_1 < t_2 < \dots < t_{p-1} < t_p < t < t_{p+1}$  such that  $\sup_\ell |t_{\ell+1} - t_\ell| = O(p^{-1})$  and the previous dynamic growth model can be approximated by its discretized version:

$$L(t_p) - L(t_1) = \sum_{\ell=1}^p (t_{\ell+1} - t_\ell) \left\{ L'_{T(t_\ell)} \circ L_{T(t_\ell)}^{-1} \circ L(t_\ell) \right\} + O(p^{-1}),$$

with  $L(t_1) = L_{T(t_1)}(t_1)$ . So, the estimator  $\widehat{L}$  of the varying temperature length profile  $L$  is defined as follows:

$$\widehat{L}(t_p) - L(t_1) = \sum_{\ell=1}^p (t_{\ell+1} - t_\ell) \left\{ \widehat{L}'_{T(t_\ell)} \circ \widehat{L}_{T(t_\ell)}^{-1} \circ \widehat{L}(t_\ell) \right\}.$$

Once the varying temperature growth profile estimated, the ultimate task is to compute the hatching time and the post mortem interval *pmi*. To this end, one observes on the crime scene at a given date  $t^*$  a sample of i.i.d. larval lengths  $Y_1^*, \dots, Y_{n_{obs}}^*$  corresponding to the growth length  $L(t^* - t_h)$  reached at time  $t^* - t_h$  ( $:= \text{pmi}$ ) after hatching and computed from the past outdoor temperature time series  $\{T(t^* - t); t \in [t_h, t^*]\}$ , where  $t_h$  stands for the unknown hatching date. Moreover, for  $i = 1, \dots, n_{obs}$ , one assumes  $Y_i^* = L(t^* - t_h) + \epsilon_i$  where the  $\epsilon_i$ 's are zero mean random errors. Then, the estimated date of hatching  $\widehat{t}_h$  is the minimizer of  $\widehat{Q}(t) := (\widehat{L}(t^* - t) - \bar{Y}^*)^2$ , which gives the estimation of the post mortem interval:  $\widehat{\text{pmi}} = t^* - \widehat{t}_h$ .

**THEOREM 4** *Under (H1)-(H8) it holds:*

$$\begin{aligned} \widehat{t}_h - t_h &= O(h_L^2) + O(h_S) + O(h_{S'}) + O(h_w) + O(h_{w'}) \\ &\quad + O(p^{-1}) + O_P \left\{ (nh_L^6)^{-1/3} \right\} + O_P \left( n_{obs}^{-1/2} \right). \end{aligned}$$

As a by-product, one gets under same assumptions the consistency of the post mortem interval:

$$\begin{aligned} \widehat{\text{pmi}} - \text{pmi} &= O(h_L^2) + O(h_S) + O(h_{S'}) + O(h_w) + O(h_{w'}) + O(p^{-1}) \\ &\quad + O_P \left\{ (nh_L^6)^{-1/3} \right\} + O_P \left( n_{obs}^{-1/2} \right). \end{aligned}$$

## 4 Empirical demonstrations

In this section, we consider first some simulation studies to assess the robustness of the proposed method to errors in the temperature profile measured at the crime scene. Then, we present the application of the method to the data coming from two investigations. For reasons of privacy, the cases have been anonymised and we conventionally set the time at which the measurements of larval lengths have been taken to be  $t^* = 0$ , with negative times indicating the hours before this moment. In both these forensic cases, we do not have an external corroboration (such as a defendant confession) of the time the body has been abandoned, therefore we compare the results of our procedure with those provided by the ADH method currently used in criminal cases.

Throughout this section, we use Gaussian kernels in the estimation of the growth shape and the warping function with the same bandwidth  $h$ , chosen as twice the maximum interval between consecutive observed experimental temperature.

### 4.1 Simulation studies

We first simulate from model (4) using a constant temperature profile  $T(t) = 10^\circ\text{C}$ , with  $t$  between  $-200$  and  $0$  hours before the time of measurement and true hatching time  $t_h = -100$ . However, the temperature is measured with an error and, to estimate the hatching time, we can only use the perturbed temperature  $\tilde{T}(t_k) = T(t_k) + \epsilon_k$  for all  $t_k \in [-200, 0]$ , where  $\epsilon_k \sim N(0, \sigma_T^2)$ . In practice, we use a hourly time grid  $t_1 = -200, \dots, t_p = 0$  to evaluate the growth curves and optimise the criterion (5).

We consider four different values for  $\sigma_T = 0.1, 0.25, 0.75, 1$ . For each value of  $\sigma_T$ , we simulate 1000 samples of 20 observed lengths and we estimate the hatching time using a perturbed temperature profile  $\tilde{T}(t_k)$ . Figure 4 shows the distributions of the estimated hatching times for the different values of  $\sigma_T$ .

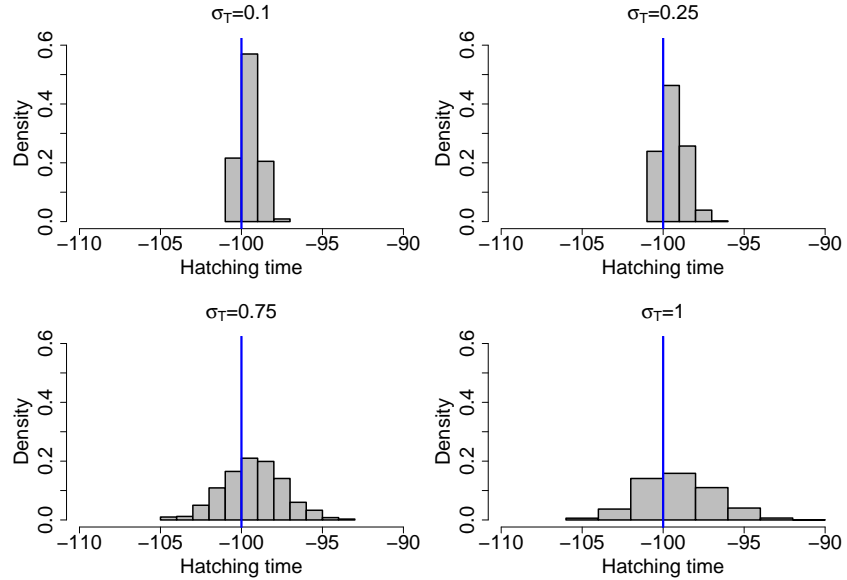


Figure 4: Histograms of the estimated hatching time over 1000 simulations when the temperature profile is measured with an error with standard deviation  $\sigma_T$ .

In practice, it is often necessary to estimate the temperature at the crime scene using the temperature measurements from the closest weather station. We consider the impact of this

procedure when the correlation between both temperatures (observed/estimated) is high ( $\rho_T = 0.9$ ) or relatively low ( $\rho_T = 0.7$ ). We simulate 250 pairs of temperatures (crime scene and weather station) from a bivariate Gaussian distribution with mean equal to  $15^\circ\text{C}$ , variance equal to 0.5 for both component and correlation  $\rho_T$ . We then use one fourth of these observation to fit a linear model between the temperature at the crime scene and the one from the weather station. Then, we simulate observed fly larvae lengths using the other crime scene temperature but we estimate the hatching time using their predicted values. Figure 5 shows the distributions of the estimated hatching times for the different values of  $\rho_T$ . While the variability of the estimator increases when the correlation decreases, the difference is not dramatic in this case. In practice, correlation between crime scene temperature data and the ones from the closest weather station is pretty high. For example, it is 0.94 in the real case described in Section 4.3.

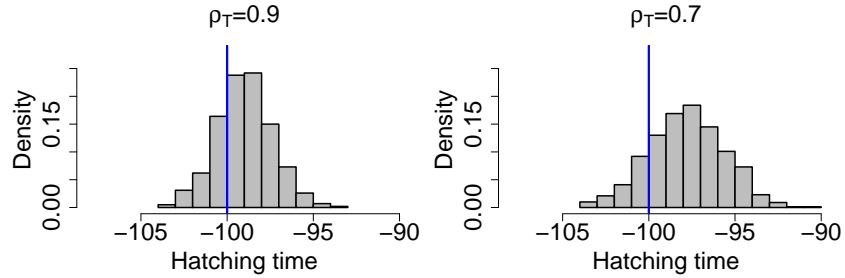


Figure 5: Histograms of the estimated hatching time over 1000 simulations when the correlation between crime scene temperature and weather station temperature is  $\rho_T$ .

We also run a simulation study with a more realistic varying temperature profile. Indeed, we consider as the true temperature profile in model (4) a subset of the temperature measurements from the weather station from the second case study in Section 4.3. For each replicate, we add to the series of temperatures an independent Gaussian error with standard deviation  $\sigma_T = 0.1, 0.25, 0.75, 1$  and we use this noisy version in the estimation of the hatching time. Figure 6 shows the distribution of the estimates for the different values of  $\sigma_T$ . It can be seen that the dispersion of the estimates increases with the error on the temperature but there is no evidence of bias.

## 4.2 First case study

We consider a first case study where  $n_{obs} = 70$  *Calliphora vicina* post-feeding larvae have been collected from the body. In this investigation, there was not a unique crime scene, since the body has been moved between death and discovery. For this reason, the temperature profile to which the body has been subjected is provided here by forensic experts, based on the information about the body location coming from the investigation. The temperature time series for the 371 hours before the time the larvae were killed, prior to subsequent measurement, together with the constant temperature growth profiles corresponding to each observed temperature in the series, can be seen in Figure 7. The interval of 371 hours was the largest one that was considered reasonable by forensic scientists at the scene.

For this case, the application of the ADH method suggested the interval between 276 and 228 hours before the measurements were taken as the most likely for the eggs to be laid on the body. The average temperature in that interval was around  $16^\circ\text{C}$ , and this would localise egg hatching between 240 and 192 hours before the measurement time (Donovan et al., 2006).

Figure 8 shows the growth curves for the hatching time estimated with (5) and the profile of the objective function in the minimisation problem. The estimated hatching time is -256 hours

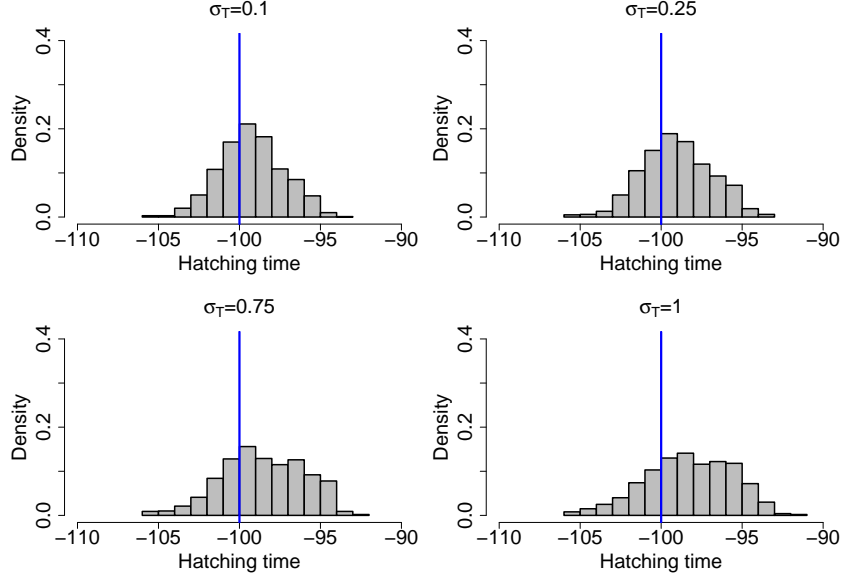


Figure 6: Histograms of the estimated hatching time over 1000 simulations when the true temperature profile is not constant and in the estimation a version corrupted by a noise with standard deviation  $\sigma_T$  is used.

(before the larval measurement), which is a bit earlier than what it was obtained from the ADH method. However, the flat plateau in the criterion suggests little stability for the estimate. Indeed, if we assume a Gaussian distribution for the measurement errors, the approximated confidence interval procedure gives us an interval of  $[-260, -190]$ , which includes the range suggested by the ADH method. Note that here the computation of the criterion is restricted to the admissible region of hatching times for which the expected growth curve would have reached the post-feeding stage by the time the larvae have been collected.

Let us now consider a few possible kinds of prior information that can be included in the estimation. The less informative prior distribution for the hatching time would be a uniform distribution between the -371-th hour and the -12th hour (the time of the body discovery). The corresponding posterior distribution obtained from (6) can be seen in Figure 9. The maximum a posteriori (MAP) estimate for the hatching time -235 hours, which is consistent with the interval provided by the ADH method. We may want instead to include in the prior the information coming from the ADH method, using a Gaussian prior distribution with mass concentrated in the interval  $[-240, -92]$  hours. In this case, the MAP provides an estimate of -221 for the hatching time. The full posterior distribution and the growth curve corresponding to the MAP estimate for the hatching time can be seen in Figure 9.

Finally, we may want to consider some problem-specific information. For example, if we want to assume that the probability of the victim to still be alive decreases progressively after their disappearance, we can use an exponential prior with mean equal to the centre of the interval provided by the ADH method. This is of course just for the sake of example and we do not claim it is necessarily a good representation of what happens in reality. The MAP of the hatching time in this case is -236 hours and the estimated growth curve, together with the posterior distribution of the hatching time, can be seen in Figure 9, bottom panel.

The primary purpose of these final examples is to show that either a frequentist or Bayesian approach can be used with the method, depending on whether there is external prior evidence available in the investigation. The choice of which methodology to use can be made based on

the evidence available and the admissibility of such evidence in court.

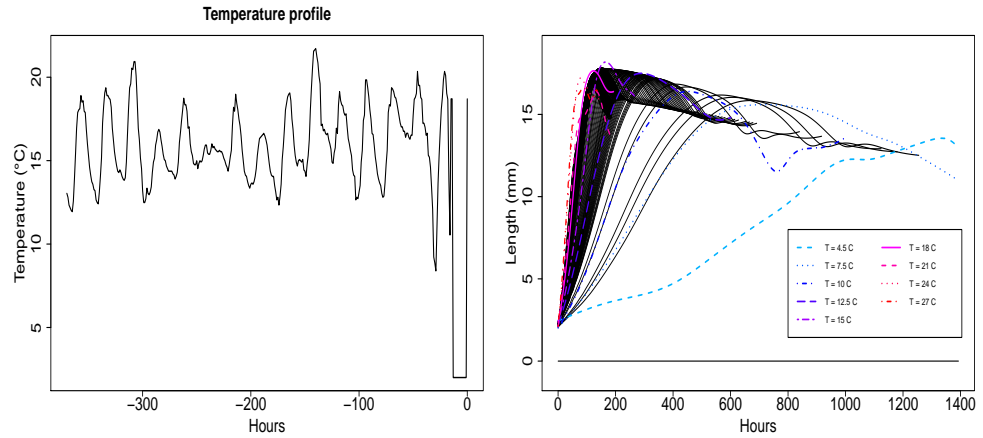


Figure 7: Left: Temperature profile to which the body has been subjected in the hours before larval lengths were measured. Note that between the body discovery and the collection of the larvae the body has been stored in a fridge for a few hours. Right: Estimated constant-temperature growth curves for each temperature in the observed interval (black lines), the temperature corresponding to observed experimental temperature are highlighted. Note the constant (zero) growth corresponding to the temperature in the fridge.

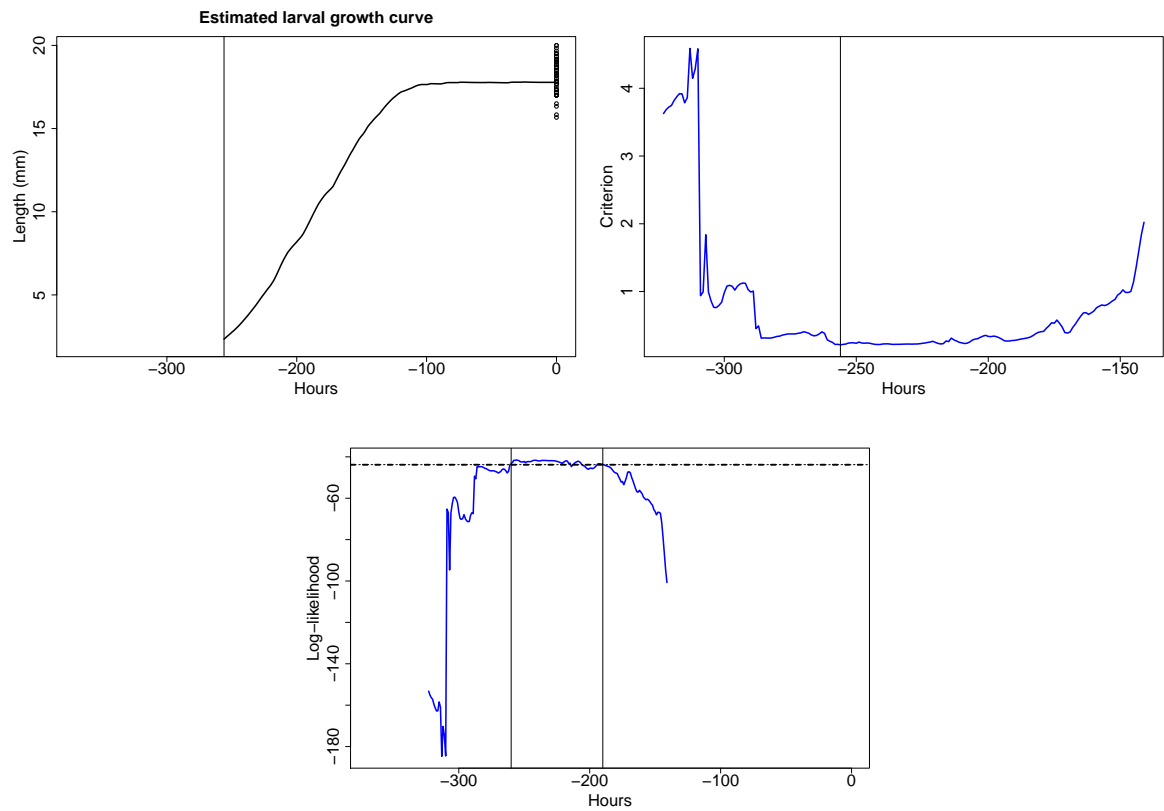


Figure 8: Top left: Estimated growth curves for the observed larvae of *Calliphora vicina*. The most likely hatching time is 250 hours before the measurements were taken. Top right: Profile of the criterion to be minimized as a function of hatching time. Bottom: Log-likelihood in the region of the estimated hatching time and boundaries of the approximated 95% confidence interval.

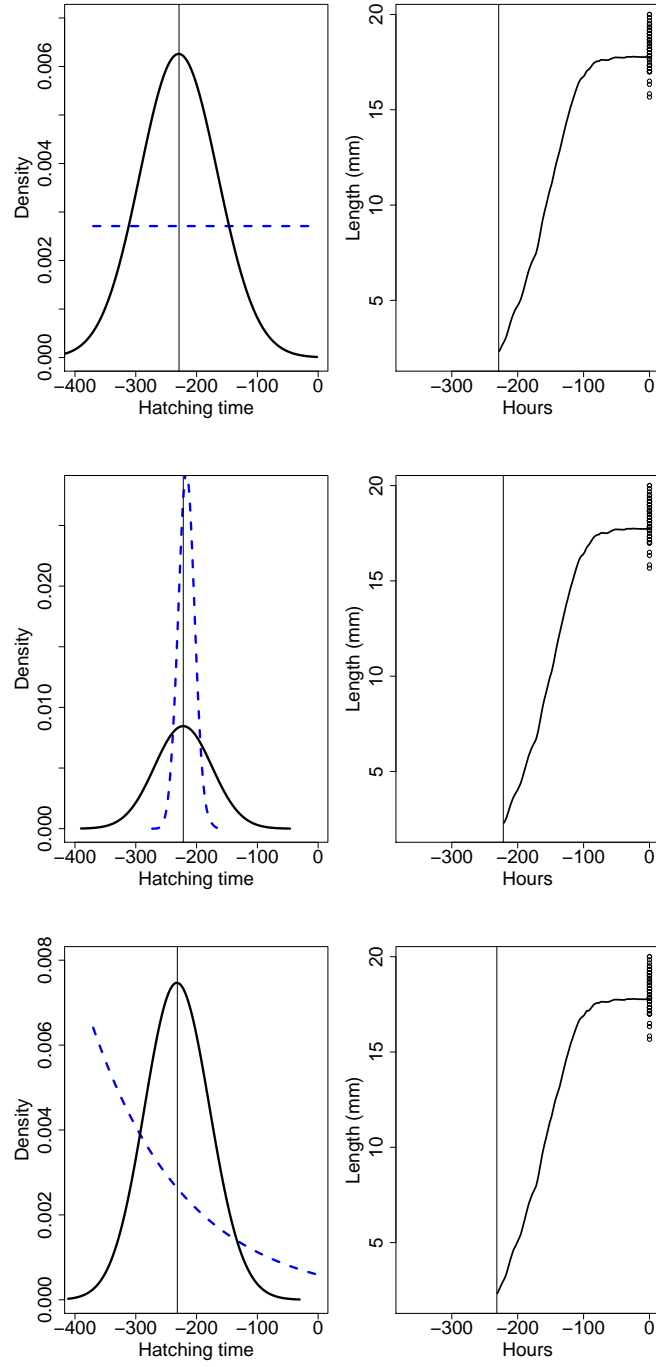


Figure 9: Left: Prior (Blue dashed line) and posterior (black solid line) distributions of the hatching time, with uniform (top), Gaussian (centre) and exponential (bottom) prior distributions for the first case study. The vertical lines denote the maximum a posteriori estimates in the three cases. Right: Expected growth curve from MAP estimates of the hatching times.

### 4.3 Second case study

In this second case study we also consider including the estimation of the temperature profile. A logger measures the temperature at the crime scene *after* the body is discovered and this is compared to the data from the closest weather station, which are used to predict the past temperature at the crime scene. In particular, we are going to use a local polynomial kernel regression to predict the crime scene temperature. The temperature at the crime scene, the weather station temperature measurements and the predicted crime scene temperature can be seen in Figure 10, together with the constant temperature growth curves for all the estimated temperature values.

At the crime scene, the lengths of 9 *Calliphora vomitoria* larvae still in the feeding phase have been measured (among other specimens, for which experimental developmental data are not currently available). We are using here the developmental data on *Calliphora vomitoria* collected at the Natural History Museum, London (Richards et al., 2017). The assessment from forensic scientists, based on the application of the ADH method as well as qualitative considerations about the other species present at the scene, is that the body has been infested by bowfly eggs between 270 and 240 hours before the body was discovered. Figure 11 shows the estimated growth curve and the profile of the objective function. The estimate for the hatching time is  $-255$  hours before the body discovery and the approximate confidence interval for a Gaussian error model is  $[-255, -249]$ . Note that  $-255$  is on the boundary of the admissible region and this may lead to questions about the validity of the confidence interval based on the likelihood ratio statistics. Moreover, we can see that the final expected length is too low with respect to the data and indeed the minimum for the criterion is reached at the boundary of the admissible region. This may suggest that the actual temperature at the crime scene was higher than predicted.

Figure 12 reports the results of the Bayesian method when the prior is taken to be either a uniform or a Gaussian centred over the interval suggested by the ADH method. The original forensic reports proposed a time immediately adjacent to the time of the victim disappearance. This was because information from the investigation about the last time the victim has been seen alive was also taken into account. We can do the same with our model by defining a uniform prior between the earliest possible hatching time after the last sighting of the victim alive and the time of discovery of the body. The results can be seen in the bottom panel of Figure 12. Our method suggests strongly the earliest possible time for the hatching, in agreement with experts' judgement. It should be noted again that the growth curve does not appear to be able to reach the observed lengths.

In conclusion, what happens in this case is that the experimental population did not develop to the average size of the larvae observed at the crime scene. This may be either because the development of larvae at the crime scene were affected by something that was not considered in the laboratory experiments (for example, larval-generated heat due to high concentration of specimens) or because the temperature at the crime scene was higher than expected during a portion of the development period. However, one useful advantage of the method is that this uncertainty can be captured in the resulting evidence.

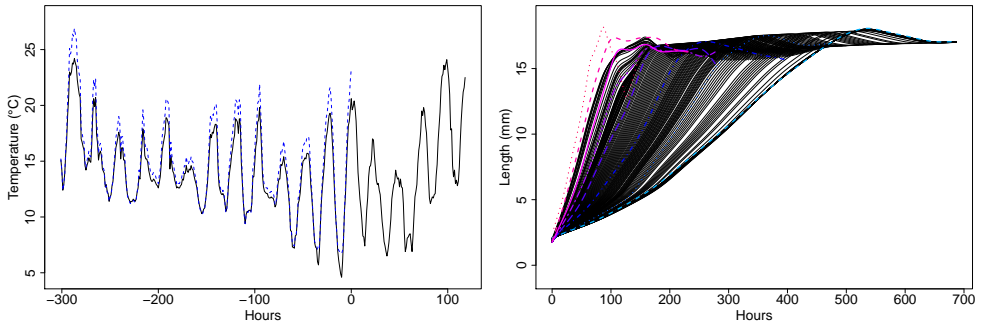


Figure 10: Left: Time series of temperature measured at the weather station closest to the crime scene (solid black line), temperature measured at the crime scene after body discovery (solid blue line) and estimated temperatures at the crime scene before body discovery (dashed blue line). Right: Estimated constant-temperature growth curves for each temperature in the observed interval.

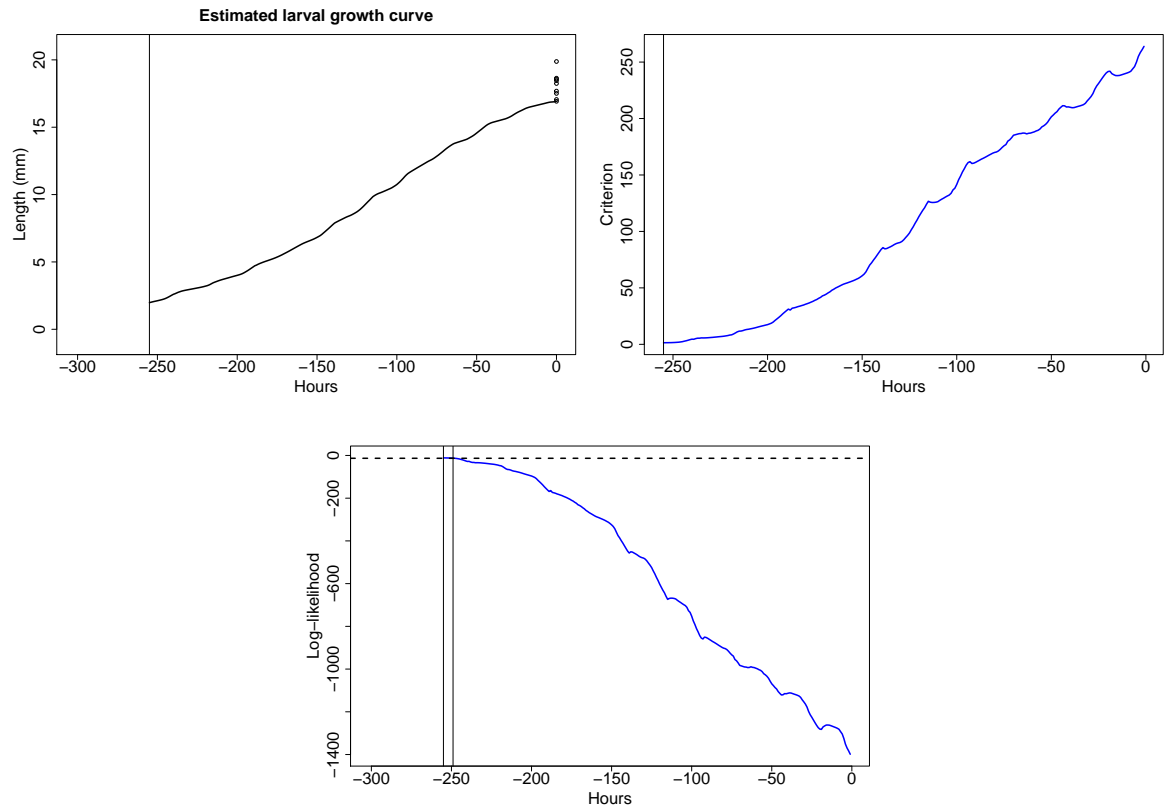


Figure 11: Top left: Estimated growth curves for the observed larvae of *Calliphora vomitoria*. The most likely hatching time is 250 hours before the measurements were taken. Top right: Profile of the criterion to be minimized as a function of hatching time. Bottom: Log-likelihood in the region of the estimated hatching time and boundaries of the approximated 95% confidence interval.

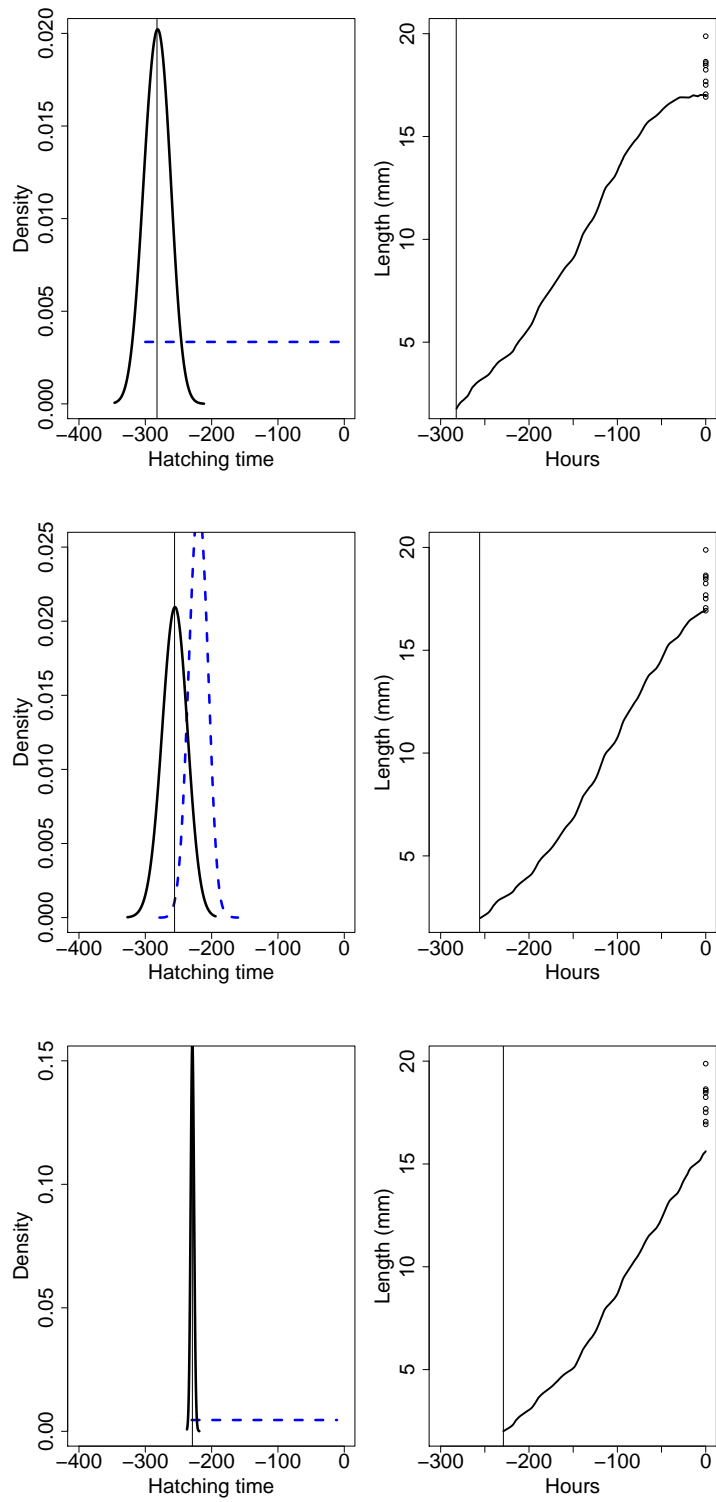


Figure 12: Left: Prior (Blue dashed line) and posterior (black solid line) distributions of the hatching time with different prior distributions, for the second case study. The vertical lines denote the maximum a posteriori estimates in the three cases. Right: Expected growth curve from MAP estimates of the hatching times.

## 5 Conclusions

We have described a functional data approach to incorporate the information from constant temperatures experimental data into the estimation of the crime scene varying temperature growth profiles. This can be later used to estimate the most likely hatching time for the observed larvae. The proposed method has some advantages with respect to existing approaches. First of all, it can be applied directly to the lengths of the larval measured at the crime scene, without the need to wait for the larvae to develop up to the next stage of the life cycle in incubators, as it is required by the ADH method. Second, the proposed method allows forensic scientists to also consider the estimated growth curve and this can be used as a model diagnostic tool to highlight any problematic situations, as seen in the second case study. Moreover, when larvae are observed in the middle of the development process, the method provides a more accurate estimate of the hatching time together with an estimate of the uncertainty. Note that this was not the case in the two case studies we considered, where larvae already reached the maximum size or they were in the post-feeding phase.

We have demonstrated both theoretically and empirically that the functional data approach can provide good estimates for the interval from hatching time to discovery of the body. These are, of course, subject to a number of uncertainties, such as those relating to temperature estimation as well as the inherent biological variability in both the experimental and crime scene entomological data. We have shown that this uncertainty can be captured both in a frequentist or Bayesian setting, allowing the model to be used in either framework, depending on the availability of additional prior knowledge and the legal requirements of the court.

It needs to be stressed that the methods by no means give a definitive conclusion about the post mortem interval on their own, since, on the one hand, many factors can delay the access of flies to the body (see, e.g., Bhadra et al., 2014) and, on the other hand, only expert judgement about the surroundings can guarantee that the observed larval specimens are the oldest to have colonised the body. However, they do yield more complete developmental estimates of the growth of the larvae compared with the simpler accumulated degree hour models, and therefore are of use in fieldwork situations. The model could also be extended to consider the interval between eggs' deposition and hatching and this is scope for future work.

## Appendix A Assumptions

Let us first start with assumptions about the constant temperature growth profile  $L_T$ , the rescaled growth shape  $S_T$ , and the warping function  $w_T$ , for any temperature  $T$ :

- (H1) For any  $T$ ,  $L_T$  is a four-times continuously differentiable function over  $(0, t_{pup})$  with a nonnull second derivative in the neighbourhood of the maximum length time: there exists  $C > 0$  and  $\delta > 0$ , such that, for all  $t \in (t_{max} - \delta, t_{max} + \delta)$ ,  $|L_T''(t)| > C$ ,
- (H2) For any  $T$ ,  $S_T$  is four-times continuously differentiable and the following uniform Lipschitz property hold: it exists  $0 < M < \infty$  such that, for any temperatures  $\tau_1$  and  $\tau_2$ ,  $\|S_{\tau_1} - S_{\tau_2}\|_{\infty} \leq M |\tau_1 - \tau_2|$  and  $\|S'_{\tau_1} - S'_{\tau_2}\|_{\infty} \leq M |\tau_1 - \tau_2|$ ,
- (H3) For simplicity and unicity purposes,  $w_T$  is assumed to be a strictly increasing 2nd degree polynomial for any  $T$  and has the uniform Lipschitz property: it exists  $0 < M < \infty$  such that, for any temperatures  $\tau_1$  and  $\tau_2$ ,  $\|w_{\tau_1} - w_{\tau_2}\|_{\infty} \leq M |\tau_1 - \tau_2|$  and  $\|w'_{\tau_1} - w'_{\tau_2}\|_{\infty} \leq M |\tau_1 - \tau_2|$ .

About the kernel functions. Let  $\mathcal{K}$  stand for  $K_L(\cdot)$ ,  $K_S(\cdot)$ ,  $K_{S'}(\cdot)$ ,  $K_w(\cdot)$  and  $K_{w'}(\cdot)$ :

(H4)  $\mathcal{K}$  is a symmetric bounded continuously differentiable kernel function on its support with  $\mathcal{K}'$  bounded such that  $\text{supp}(\mathcal{K}) = (-1, 1)$ ,  $\int \mathcal{K}(u) du = 1$ .

About the variability of the observed  $Y_{kjl}$ 's for any  $k = 1, 2, \dots, K$ :

(H5) Set  $\sigma_k^2(t_j^k) := \text{Var}(\bar{Y}_{kj})$ ;  $\sigma_k^2(\cdot)$  is an integrable and continuously differentiable function.

About the weighted function  $\omega_k(\cdot)$ 's involved in the linear local mean squared minimization problem:

(H6) For any  $k = 1, \dots, K$ ,  $\omega_k(\cdot)$  is a twice continuously differentiable function.

About the sample sizes, grid sizes and the bandwidths used in the estimating procedure, one requests:

(H7) let  $n := \inf_k n_k$ ;  $n$  tends to infinity,  $h_L$  tends to zero with  $n$ , and  $n h_L^6$  tends to infinity with  $n$ ,

(H8) the grid size  $K$  tends to infinity;  $h_S, h_{S'}, h_w$ , and  $h_{w'}$  tends to zero with  $K$ ;  $p$  tends to infinity.

## Appendix B Details of proofs

### B.1 Proof of Theorem 1

Let  $\tau_1^k < \dots < \tau_{N_\epsilon}^k$  be a grid of size  $N_\epsilon$  such that  $\cup_{l=1}^{N_\epsilon} (\tau_l^k - \epsilon, \tau_l^k + \epsilon)$  is a covering of  $[0, t_{pup}^k]$  and for any  $t$  in  $[0, t_{pup}^k]$ , define  $\ell(t) := \arg \min_{\ell \in \{1, \dots, N_\epsilon\}} |t - \tau_\ell^k|$ . The uniform rate of convergence of  $\tilde{L}_{T_k}$  is based on the decomposition:

$$\begin{aligned} \sup_t |\tilde{L}_{T_k}(t) - L_{T_k}(t)| &\leq \underbrace{\sup_t |\tilde{L}_{T_k}(t) - \tilde{L}_{T_k}(\tau_{\ell(t)})|}_{T_1} + \underbrace{\sup_t |\tilde{L}_{T_k}(\tau_{\ell(t)}) - E\tilde{L}_{T_k}(\tau_{\ell(t)})|}_{T_2} \\ &\quad + \underbrace{\sup_t |E\tilde{L}_{T_k}(\tau_{\ell(t)}) - E\tilde{L}_{T_k}(t)|}_{T_3} + \underbrace{\sup_t |E\tilde{L}_{T_k}(t) - L_{T_k}(t)|}_{T_4} \end{aligned} \quad (12)$$

About  $T_1$ . According to the definition of  $\tilde{L}_{T_k}$ , one has:

$$\begin{aligned} \tilde{L}_{T_k}(t) - \tilde{L}_{T_k}(\tau_{\ell(t)}) &= \frac{s_2(t)s_0^Y(t) - s_1(t)s_1^Y(t)}{s_0(t)s_2(t) - s_1(t)^2} - \frac{s_2(\tau_{\ell(t)})s_0^Y(\tau_{\ell(t)}) - s_1(\tau_{\ell(t)})s_1^Y(\tau_{\ell(t)})}{s_0(\tau_{\ell(t)})s_2(\tau_{\ell(t)}) - s_1(\tau_{\ell(t)})^2} \\ &= \frac{A}{B} - \frac{A_\tau}{B_\tau} \\ &= \frac{(A - A_\tau)B_\tau - (B - B_\tau)A_\tau}{BB_\tau}, \end{aligned} \quad (13)$$

where, for  $m = 0, 1, 2$  and for any  $t$ ,  $s_m(t) := \sum_{j=1}^{n_k} \omega_k(t_j)(t_j - t)^m K_L \{h_L^{-1}(t_j - t)\}$  and for  $m = 0, 1$ ,  $s_m^Y(t) := \sum_{j=1}^{n_k} \omega_k(t_j)(t_j - t)^m K_L \{h_L^{-1}(t_j - t)\} \bar{Y}_{kj}$ . A straightforward calculus leads to the following writings:

$$\begin{aligned} |A - A_\tau| &\leq |s_2(t) - s_2(\tau_{\ell(t)})| |s_0^Y(t)| + |s_0^Y(t) - s_0^Y(\tau_{\ell(t)})| |s_2(\tau_{\ell(t)})| \\ &\quad + |s_1(t) - s_1(\tau_{\ell(t)})| |s_1^Y(t)| + |s_1^Y(t) - s_1^Y(\tau_{\ell(t)})| |s_1(\tau_{\ell(t)})|, \end{aligned} \quad (14)$$

and

$$\begin{aligned} |B - B_\tau| &\leq |s_2(t) - s_2(\tau_{\ell(t)})| |s_0(\tau_{\ell(t)})| + |s_0(t) - s_0(\tau_{\ell(t)})| |s_2(t)| \\ &\quad + |s_1(t) - s_1(\tau_{\ell(t)})| |s_1(t) + s_1(\tau_{\ell(t)})|. \end{aligned} \quad (15)$$

By involving kernel properties, taylor expansion, and numerical integral approximation, one is able to state:

- (a)  $s_0(t) = \nu(t) n_k h_L + O(n_k h_L^3),$
- (b)  $s_1(t) = \nu'(t) n_k h_L^3 \int y^2 K(y) dy + O(n_k h_L^5),$
- (c)  $s_2(t) = \nu(t) n_k h_L^3 \int y^2 K_L(y) dy + O(n_k h_L^5),$
- (d)  $s_0^Y(t) = O_P(n_k h_L),$
- (e)  $s_1^Y(t) = O_P(n_k h_L^3),$
- (f)  $s_0(t) - s_0(\tau_{\ell(t)}) = O(n_k h_L^{-1} \epsilon),$
- (g)  $s_1(t) - s_1(\tau_{\ell(t)}) = O(n_k \epsilon),$
- (h)  $s_2(t) - s_2(\tau_{\ell(t)}) = O(n_k h_L \epsilon),$
- (i)  $s_0^Y(t) - s_0^Y(\tau_{\ell(t)}) = O_P(n_k h_L^{-1} \epsilon),$
- (j)  $s_1^Y(t) - s_1^Y(\tau_{\ell(t)}) = O_P(n_k \epsilon).$

*Proof of (b).* By numerical approximation and (H6), one has

$$\begin{aligned} s_1(t) &= n_k \int w_k(u)(u-t) K_L\{h_L^{-1}(u-t)\} + O(1) \\ &= n_k h_L^2 \int y K_L(y) w_k(t+hy) dy + O(1) \\ &= w'_k(t) n_k h_L^3 \int y^2 K_L(y) dy + O(n_k h_L^5), \end{aligned}$$

the last equality using the taylor expansion of  $\omega_k$  and  $\int y K_L(y) dy = 0$ .

*Proof of (a).* Just follow the same steps without the term  $(t_j - t)^2$ .

*Proof of (c).* This proof is very similar to the previous one:

$$\begin{aligned} s_2(t) &= n_k \int w_k(u)(u-t)^2 K_L\{h_L^{-1}(u-t)\} + O(1) \\ &= n_k h_L^3 \int y^2 K_L(y) w_k(t+hy) dy + O(1) \\ &= w_k(t) n_k h_L^3 \int y^2 K_L(y) dy + O(n_k h_L^3), \end{aligned}$$

*Proof of (e).* According to (H6) and (H5), one can write:

$$\begin{aligned}
Var \{s_1^Y(t)\} &= \sum_{j=1}^{n_k} \omega_k(t_j)(t_j - t)^2 K_L^2 \{h_L^{-1}(t_j - t)\} \sigma^2(t_j) \\
&= n_k \int \omega_k(u)(u - t)^2 K_L^2 \{h_L^{-1}(u - t)\} \sigma^2(u) du + O(1) \\
&= n_k h_L^3 \int y^2 K_L^2(y) \omega_k(t + hy) \sigma^2(t + hy) dy + o(n_k h_L^3), \\
&= \omega_k(t) \sigma^2(t) n_k h_L^3 \int y^2 K_L^2(y) dy + o(n_k h_L^3).
\end{aligned} \tag{16}$$

Now, let us focus on the expectation of  $s_1^Y(t)$ :

$$\begin{aligned}
E \{s_1^Y(t)\} &= \sum_{j=1}^{n_k} \omega_k(t_j)(t_j - t) K_L \{h_L^{-1}(t_j - t)\} L_{T_k}(t_j) \\
&= n_k \int \omega_k(u)(u - t) K_L \{h_L^{-1}(u - t)\} L_{T_k}(u) du + O(1) \\
&= \{\omega_k(t) L_{T_k}(t)\}' n_k h_L^3 \int y^2 K_L^2(y) dy + o(n_k h_L^3).
\end{aligned} \tag{17}$$

So, (16) and (17) implies (e).

*Proof of (d).* By adapting the same steps to  $s_0^Y(t)$ , one gets straightforwardly (d).

*Proof of (h).* According to the definition of  $s_2(t)$ , one can write:

$$\begin{aligned}
|s_2(t) - s_2(\tau_{\ell(t)})| &= \left| \sum_{j=1}^{n_k} \omega_k(t_j) [(t_j - t)^2 K_L \{h_L^{-1}(t_j - t)\} - (t_j - \tau_{\ell(t)})^2 K_L \{h_L^{-1}(t_j - \tau_{\ell(t)})\}] \right| \\
&\leq \sum_{j=1}^{n_k} \omega_k(t_j) (t_j - t)^2 |K_L \{h_L^{-1}(t_j - t)\} - K_L \{h_L^{-1}(t_j - \tau_{\ell(t)})\}| \\
&\quad + \sum_{j=1}^{n_k} \omega_k(t_j) (t - \tau_{\ell(t)})^2 K_L \{h_L^{-1}(t_j - \tau_{\ell(t)})\} \\
&\quad + 2 \sum_{j=1}^{n_k} \omega_k(t_j) |t - \tau_{\ell(t)}| |t_j - \tau_{\ell(t)}| K_L \{h_L^{-1}(t_j - \tau_{\ell(t)})\} \\
&\leq C_1 n_k h_L \epsilon + \omega_k(t) n_k h_L \epsilon^2 + 2 \omega_k(t) n_k h_L^2 \epsilon + o(n_k h_L \epsilon),
\end{aligned}$$

the last inequality coming from standard numerical approximation. This results in:

$$|s_2(t) - s_2(\tau_{\ell(t)})| = O(n_k h_L \epsilon) \tag{18}$$

*Proof of (f)-(g).* The proofs of (f) and (g) are a direct adaptation of the previous one and hence are omitted.

*Proof of (i)-(j).* Let us start with (j). According to the definition of  $s_1^Y(t)$ , one has:

$$\begin{aligned}
& \text{Var} \{ s_1^Y(t) - s_1^Y(\tau_{\ell(t)}) \} \\
&= \sum_{j=1}^{n_k} \omega_k(t_j) [(t_j - t) K_L \{ h_L^{-1}(t_j - t) \} - (t_j - \tau_{\ell(t)}) K_L \{ h_L^{-1}(t_j - \tau_{\ell(t)}) \}]^2 \sigma^2(t_j) \\
&\leq \sum_{j=1}^{n_k} \omega_k(t_j) (t_j - t)^2 (K_L \{ h_L^{-1}(t_j - t) \} - K_L \{ h_L^{-1}(t_j - \tau_{\ell(t)}) \})^2 \sigma^2(t_j) \\
&\quad + \sum_{j=1}^{n_k} \omega_k(t_j) (t - \tau_{\ell(t)})^2 K_L \{ h_L^{-1}(t_j - \tau_{\ell(t)}) \} \sigma^2(t_j) \\
&\leq C \epsilon^2 \sum_{j=1}^{n_k} \omega_k(t_j) \sigma^2(t_j) + \epsilon^2 \sum_{j=1}^{n_k} \omega_k(t_j) K_L \{ h_L^{-1}(t_j - \tau_{\ell(t)}) \} \sigma^2(t_j).
\end{aligned}$$

Now, by using numerical approximation,  $\text{Var} \{ s_1^Y(t) - s_1^Y(\tau_{\ell(t)}) \} \leq C n_k \epsilon^2 + C' n_k h_L \epsilon^2$ , which implies that

$$\text{Var} \{ s_1^Y(t) - s_1^Y(\tau_{\ell(t)}) \} = O(n_k \epsilon^2). \quad (19)$$

Let us now focus on the expectation of  $s_1^Y(t) - s_1^Y(\tau_{\ell(t)})$ :

$$\begin{aligned}
& E \{ s_1^Y(t) - s_1^Y(\tau_{\ell(t)}) \} \\
&= \sum_{j=1}^{n_k} \omega_k(t_j) [(t_j - t) K_L \{ h_L^{-1}(t_j - t) \} - (t_j - \tau_{\ell(t)}) K_L \{ h_L^{-1}(t_j - \tau_{\ell(t)}) \}] L(t_j) \\
&\leq \sum_{j=1}^{n_k} \omega_k(t_j) |t_j - t| |K_L \{ h_L^{-1}(t_j - t) \} - K_L \{ h_L^{-1}(t_j - \tau_{\ell(t)}) \}| L(t_j) \\
&\quad + \sum_{j=1}^{n_k} \omega_k(t_j) |t - \tau_{\ell(t)}| |K_L \{ h_L^{-1}(t_j - \tau_{\ell(t)}) \}| L(t_j).
\end{aligned}$$

By using again numerical approximation, one gets

$$E \{ s_1^Y(t) - s_1^Y(\tau_{\ell(t)}) \}^2 = O \{ (n_k)^2 \epsilon^2 \}. \quad (20)$$

(19) and (20) implies (j). Concerning (i), it suffices to adapt similar steps but in a simpler way to deduce the claimed result.

Finally, (a)-(j) imply that  $A - A_\tau = O_P((n_k)^2 h_L^2 \epsilon)$ ,  $B = \omega_k(t)^2 (n_k)^2 h_L^4 \int y^2 K_L(y) dy + o \{ (n_k)^2 h_L^4 \}$ ,  $B - B_\tau = O((n_k)^2 h_L^2 \epsilon)$ , and  $B_\tau = \omega_k(\tau_{\ell(t)})^2 (n_k)^2 h_L^4 \int y^2 K_L(y) dy + o \{ (n_k)^2 h_L^4 \}$ . So, (13)-(15) allow us to get  $\tilde{L}_{T_k}(t) - \tilde{L}_{T_k}(\tau_{\ell(t)}) = O_P(h^{-2} \epsilon)$ . As this property holds uniformly on  $t$ , it comes:

$$\sup_t |\tilde{L}_{T_k}(t) - \tilde{L}_{T_k}(\tau_{\ell(t)})| = O_P(h^{-2} \epsilon). \quad (21)$$

*About  $T_3$ .* The asymptotic behaviour of  $T_3$  can be derived from  $T_1$ :

$$\begin{aligned}
\sup_t |E \tilde{L}_{T_k}(t) - E \tilde{L}_{T_k}(\tau_{\ell(t)})| &\leq \sup_t E |\tilde{L}_{T_k}(t) - \tilde{L}_{T_k}(\tau_{\ell(t)})| \\
&\leq E \sup_t |\tilde{L}_{T_k}(t) - \tilde{L}_{T_k}(\tau_{\ell(t)})|.
\end{aligned}$$

So, (21) implies that

$$\sup_t |E \tilde{L}_{T_k}(t) - E \tilde{L}_{T_k}(\tau_{\ell(t)})| = O_P(h^{-2} \epsilon). \quad (22)$$

About  $T_2$ . According to the definition of  $\tilde{L}_{T_k}(\tau_{\ell(t)})$ , one has:

$$\frac{\tilde{L}_{T_k}(\tau_{\ell(t)}) - E\tilde{L}_{T_k}(\tau_{\ell(t)})}{s_2(\tau_{\ell(t)}) \{s_0^Y(\tau_{\ell(t)}) - Es_0^Y(\tau_{\ell(t)})\} - s_1(\tau_{\ell(t)}) \{s_1^Y(\tau_{\ell(t)}) - Es_1^Y(\tau_{\ell(t)})\}} = \frac{s_2(\tau_{\ell(t)}) \{s_0^Y(\tau_{\ell(t)}) - Es_0^Y(\tau_{\ell(t)})\} - s_1(\tau_{\ell(t)}) \{s_1^Y(\tau_{\ell(t)}) - Es_1^Y(\tau_{\ell(t)})\}}{s_0(\tau_{\ell(t)})s_2(\tau_{\ell(t)}) - s_1(\tau_{\ell(t)})^2}. \quad (23)$$

(16) implies that  $E \{s_1^Y(\tau_{\ell(t)}) - Es_1^Y(\tau_{\ell(t)})\}^2 = Var \{s_1^Y(\tau_{\ell(t)})\} = O(n_k h_L^3)$ . In a similar way, it is easy to see  $E \{s_0^Y(\tau_{\ell(t)}) - Es_0^Y(\tau_{\ell(t)})\}^2 = Var \{s_0^Y(\tau_{\ell(t)})\} = O(n_k h_L)$ . These results with (a)-(c) and (23) lead to the standard rate:

$$\tilde{L}_{T_k}(\tau_{\ell(t)}) - E\tilde{L}_{T_k}(\tau_{\ell(t)}) = O_P \{(n_k h_L)^{-1/2}\}. \quad (24)$$

In addition, one can write:

$$\begin{aligned} P \left( \sup_t \left| \tilde{L}_{T_k}(\tau_{\ell(t)}) - E\tilde{L}_{T_k}(\tau_{\ell(t)}) \right| > \eta \right) &= P \left( \max_\ell \left| \tilde{L}_{T_k}(\tau_{\ell(t)}) - E\tilde{L}_{T_k}(\tau_{\ell(t)}) \right| > \eta \right) \\ &\leq N_\epsilon \max_\ell P \left( \left| \tilde{L}_{T_k}(\tau_{\ell(t)}) - E\tilde{L}_{T_k}(\tau_{\ell(t)}) \right| > \eta \right). \end{aligned}$$

Because  $N_\epsilon = O(\epsilon^{-1})$  and (24), it comes:

$$\sup_t \left| \tilde{L}_{T_k}(\tau_{\ell(t)}) - E\tilde{L}_{T_k}(\tau_{\ell(t)}) \right| = O_P \{(n_k h_L \epsilon)^{-1/2}\}. \quad (25)$$

About  $T_4$ .

$$E\tilde{L}_{T_k}(t) - L_{T_k}(t) = \frac{s_2(t)s_0^{DL}(t) - s_1(t)s_1^{DL}(t)}{s_0(t)s_2(t) - s_1(t)^2},$$

where, for  $m = 0, 1$ ,  $s_m^{DL}(t) := \sum_{j=1}^{n_k} \omega_k(t_j)(t_j - t)^m K_L \{h_L^{-1}(t_j - t)\} \{L_{T_k}(t_j) - L_{T_k}(t)\}$ . Accord-

ing to the regularity assumptions on  $L_{T_k}$ , it is easy to show that  $s_0^{DL}(t) = O(n_k h_L^3)$  as well as  $s_1^{DL}(t) = O(n_k h_L^3)$ . So, as soon as  $\epsilon = o(h^2)$ , one has:

$$E\tilde{L}_{T_k}(\tau_{\ell(t)}) - L_{T_k}(t) = O(h_L^2). \quad (26)$$

(12), (21), (22), (25), and (26) provide the claimed result:

$$\sup_t \left| \tilde{L}_{T_k}(t) - L_{T_k}(t) \right| = O_P(h_L^{-2}\epsilon) + O_P \{(n h_L \epsilon)^{-1/2}\} + O(h_L^2).$$

Choosing  $\epsilon = h_L n^{-1/3}$  for balancing both  $O_P$  leads to the claimed result:

$$\left\| \tilde{L}_{T_k} - L_{T_k} \right\|_\infty = O(h_L^2) + O_P \{(n h_L^3)^{-1/3}\}.$$

Let us now focus on the local linear estimator  $\tilde{L}'_{T_k}(t)$  of the derivative of  $L'(t)$ . To derive the uniform rate of convergence, we adapt the previous result. To this end, we replace  $L_{T_k}$  with  $L'_{T_k}$ ,  $\tilde{L}_{T_k}$  with

$$\tilde{L}'_{T_k}(t) = \frac{s_0(t)s_1^Y(t) - s_1(t)s_0^Y(t)}{B},$$

$A$  with  $A' = s_0(t)s_1^Y(t) - s_1(t)s_0^Y(t)$ , and  $\omega_k(t_j)$  with  $A'_\tau = s_0(\tau_{\ell(t)})s_1^Y(\tau_{\ell(t)}) - s_1(\tau_{\ell(t)})s_0^Y(\tau_{\ell(t)})$ . In this way, it is easy to see that

$$\begin{aligned} |A' - A'_\tau| &\leq |s_0(t) - s_0(\tau_{\ell(t)})| |s_1^Y(t)| + |s_1^Y(t) - s_1^Y(\tau_{\ell(t)})| |s_0(\tau_{\ell(t)})| \\ &\quad + |s_1(t) - s_1(\tau_{\ell(t)})| |s_0^Y(t)| + |s_0^Y(t) - s_0^Y(\tau_{\ell(t)})| |s_1(\tau_{\ell(t)})|. \end{aligned}$$

So, by using (a)-(b), (d)-(e), and (f)-(g), one gets  $A' - A'_\tau = O_P(n h_L \epsilon)$ , and by using similar arguments as previously, it comes:

$$\sup_t \left| \tilde{L}'_{T_k}(t) - \tilde{L}'_{T_k}(\tau_{\ell(t)}) \right| = O_P(h_L^{-3} \epsilon), \quad (27)$$

and

$$\sup_t \left| E \tilde{L}'_{T_k}(t) - E \tilde{L}'_{T_k}(\tau_{\ell(t)}) \right| = O_P(h_L^{-3} \epsilon). \quad (28)$$

Let us now consider the quantity

$$\begin{aligned} & \tilde{L}'_{T_k}(\tau_{\ell(t)}) - E \tilde{L}'_{T_k}(\tau_{\ell(t)}) \\ &= \frac{s_0(\tau_{\ell(t)}) \{s_1^Y(\tau_{\ell(t)}) - Es_1^Y(\tau_{\ell(t)})\} - s_1(\tau_{\ell(t)}) \{s_0^Y(\tau_{\ell(t)}) - Es_0^Y(\tau_{\ell(t)})\}}{B_\tau}. \end{aligned}$$

Remember that  $Var\{s_1^Y(\tau_{\ell(t)})\} = O(n_k h_L^3)$ ,  $Var\{s_0^Y(\tau_{\ell(t)})\} = O(n_k h_L)$ , and  $B_\tau = C \omega_k(\tau_{\ell(t)})^2 (n_k)^2 h_L^4 + o\{(n_k)^2 h_L^4\}$ . These results combined with (a)-(b) and (i)-(j) imply that  $\tilde{L}'_{T_k}(\tau_{\ell(t)}) - E \tilde{L}'_{T_k}(\tau_{\ell(t)}) = O_P\{(n_k h_L^3)^{-1/2}\}$ , which results in

$$\sup_t \left| \tilde{L}'_{T_k}(\tau_{\ell(t)}) - E \tilde{L}'_{T_k}(\tau_{\ell(t)}) \right| = O_P\{(n_k h_L^3 \epsilon)^{-1/2}\}. \quad (29)$$

About the bias term, one can write  $E \tilde{L}'_{T_k}(t) - L'_{T_k}(t) = D/B$  with

$$D = s_0(t) \{s_1^L(t) - s_2(t)L'(t)\} - s_1(t) \{s_0^L(t) - s_1(t)L'(t)\},$$

where, for  $m = 0, 1$ ,  $s_m^L(t) := \sum_{j=1}^{n_k} \omega_k(t_j) (t_j - t)^m K_L\{h_L^{-1}(t_j - t)\} L_{T_k}(t_j)$ . By using taylor expansions, it comes that

$$s_0^L(t) - s_1(t)L'(t) = w(t)L(t) n h_L + C_1 n h_L^3 + O(n h_L^5),$$

and

$$s_1^L(t) - s_2(t)L'(t) = w'(t)L(t) n h_L^3 \int y^2 K_L(y) dy + O(n h_L^5).$$

By gathering previous results, the main term of  $D$  vanishes and one gets

$$\sup_t \left| E \tilde{L}'_{T_k}(t) - L'_{T_k}(t) \right| = O(h_L^2).$$

Finally, the last result with (27)-(29) gives the uniform rate of convergence of  $L'_{T_k}$ :

$$\left\| \tilde{L}'_{T_k} - L'_{T_k} \right\|_\infty = O_P(h_L^{-3} \epsilon) + O_P\{(n_k h_L^3 \epsilon)^{-1/2}\} + O(h_L^2).$$

Choosing  $\epsilon = h_L n^{-1/3}$  for balancing both  $O_P$  leads to the claimed result:

$$\left\| \tilde{L}'_{T_k} - L'_{T_k} \right\|_\infty = O(h_L^2) + O_P\{(n h_L^6)^{-1/3}\}.$$

## B.2 Proof of Theorem 2

Let us first derive asymptotic behaviour of the rescaled growth shape  $\tilde{S}_{T_k}$  and the warping function  $\tilde{w}_{T_k}$  corresponding to a constant temperature  $T_k$ . For any temperature  $T_k$ , it is easy to see that  $\tilde{S}_{T_k}$  inherits in some sense the asymptotic properties of  $\tilde{L}_{T_k}$  and  $\tilde{w}_{T_k}$ . First,  $w_{T_k}$  (resp.  $\tilde{w}_{T_k}$ ) is a strictly increasing function; so its inverse function  $w_{T_k}^{-1}$  (resp.  $\tilde{w}_{T_k}^{-1}$ ) is well defined. Secondly, for any  $u \in [0, 1]$  and for any temperature  $T_k$ , one has

$$\begin{aligned} & |\tilde{S}_{T_k}(u) - S_{T_k}(u)| \\ &= \left| \tilde{L}_{T_k} \left\{ \tilde{w}_{T_k}^{-1}(u) \right\} - L_{T_k} \left\{ w_{T_k}^{-1}(u) \right\} \right|, \\ &\leq \left| \tilde{L}_{T_k} \left\{ \tilde{w}_{T_k}^{-1}(u) \right\} - L_{T_k} \left\{ \tilde{w}_{T_k}^{-1}(u) \right\} \right| + \left| L_{T_k} \left\{ \tilde{w}_{T_k}^{-1}(u) \right\} - L_{T_k} \left\{ w_{T_k}^{-1}(u) \right\} \right|. \end{aligned}$$

So, according to the smoothness assumption (H1) of  $L_{T_k}$ , it exists  $C > 0$  such that:

$$\left\| \tilde{S}_{T_k} - S_{T_k} \right\|_{\infty} \leq \left\| \tilde{L}_{T_k} - L_{T_k} \right\|_{\infty} + C \left\| \tilde{w}_{T_k}^{-1} - w_{T_k}^{-1} \right\|_{\infty}. \quad (30)$$

For any  $u \in [0, 1]$ , it exists  $t \in [0, t_{pup}^k]$  such that  $u = \tilde{w}_{T_k}(t)$ :

$$\begin{aligned} \left| \tilde{w}_{T_k}^{-1}(u) - w_{T_k}^{-1}(u) \right| &= \left| t - w_{T_k}^{-1} \{ \tilde{w}_{T_k}(t) \} \right|, \\ &= \left| w_{T_k}^{-1} \{ w_{T_k}(t) \} - w_{T_k}^{-1} \{ \tilde{w}_{T_k}(t) \} \right|. \end{aligned}$$

Moreover, thanks to (H3)  $w_{T_k}$  is a one-to-one twice differentiable function, its inverse function  $w_{T_k}^{-1}$  has the standard Lipschitz property. So, it exists  $C > 0$  such that:

$$\left| w_{T_k}^{-1}(u_1) - w_{T_k}^{-1}(u_2) \right| \leq C |u_1 - u_2|. \quad (31)$$

By combining (30) with (31) it comes:

$$\left\| \tilde{S}_{T_k} - S_{T_k} \right\|_{\infty} \leq \left\| \tilde{L}_{T_k} - L_{T_k} \right\|_{\infty} + C \left\| \tilde{w}_{T_k} - w_{T_k} \right\|_{\infty}. \quad (32)$$

Let us now focus on the asymptotic behaviour of  $\tilde{w}_{T_k}$ . We remind that  $\tilde{w}_{T_k}$  is a strictly increasing quadratic polynomial such that  $\tilde{w}_{T_k}(0) = 0$ ,  $\tilde{w}_{T_k}(\tilde{t}_{max}^k) = \alpha$ ,  $\tilde{w}_{T_k}(t_{pup}^k) = 1$ , where  $\tilde{t}_{max}^k = \arg \sup_t \tilde{L}_{T_k}(t)$ . Here, the pupation time is assumed to be the same for both  $L_{T_k}$  and  $\tilde{L}_{T_k}$ . By using a standard Taylor expansion of  $L'_{T_k}$  and the fact that the derivative vanishes where the maximum is reached (i.e.  $L'_{T_k}(t_{max}^k) = 0$ ), it exists  $t^*$  in  $(\min(t_{max}^k, \tilde{t}_{max}^k), \max(t_{max}^k, \tilde{t}_{max}^k))$  such that:

$$L'_{T_k}(\tilde{t}_{max}^k) = (\tilde{t}_{max}^k - t_{max}^k) L''_{T_k}(t^*),$$

with  $|L''_{T_k}(t^*)|$  lower bounded by a nonnegative constant thanks to (H1). Because  $\tilde{t}_{max}^k$  is the maximum length reached by  $\tilde{L}_{T_k}$ , one has  $\tilde{L}'_{T_k}(\tilde{t}_{max}^k) = 0$  and one gets  $L'_{T_k}(\tilde{t}_{max}^k) - \tilde{L}'_{T_k}(\tilde{t}_{max}^k) = (\tilde{t}_{max}^k - t_{max}^k) L''_{T_k}(t^*)$ . As a by-product  $\tilde{t}_{max}^k$  inherits the asymptotic properties of  $\tilde{L}'_{T_k}$ :

$$\tilde{t}_{max}^k = t_{max}^k + O(h_L^2) + O_P \left( \{n h_L^6\}^{-1/3} \right). \quad (33)$$

Now remember that  $w_{T_k}$  (resp.  $w_{T_k}$  and  $\tilde{w}_{T_k}$ ) is an interpolating quadratic polynomial. So, it is easy to see that the variations between  $w_{T_k}$  and  $\tilde{w}_{T_k}$  is controlled by the rate of convergence of  $\tilde{t}_{max}^k - t_{max}^k$ . Let  $\mathbf{W}$  and  $\tilde{\mathbf{W}}$  be the  $2 \times 2$ -matrices:

$$\mathbf{W} = \begin{pmatrix} t_{max}^k & (t_{max}^k)^2 \\ t_{pup}^k & (t_{pup}^k)^2 \end{pmatrix} \text{ and } \tilde{\mathbf{W}} = \begin{pmatrix} \tilde{t}_{max}^k & (\tilde{t}_{max}^k)^2 \\ t_{pup}^k & (t_{pup}^k)^2 \end{pmatrix}.$$

Because  $t_{max}^k \neq t_{pup}^k$  and  $\tilde{t}_{max}^k \neq t_{pup}^k$ ,  $\mathbf{W}$  and  $\widetilde{\mathbf{W}}$  are two invertible matrices, one can write  $w_{T_k}(t) = (t, t^2) \mathbf{W}^{-1} \begin{pmatrix} \alpha \\ 1 \end{pmatrix}$  and  $\tilde{w}_{T_k}(t) = (t, t^2) \widetilde{\mathbf{W}}^{-1} \begin{pmatrix} \alpha \\ 1 \end{pmatrix}$  and it comes:

$$\begin{aligned} \sup_{t \in [0, t_{pup}^k]} |\tilde{w}_{T_k}(t) - w_{T_k}(t)| &= \sup_{t \in [0, t_{pup}^k]} \left\| (t, t^2) \left( \widetilde{\mathbf{W}}^{-1} - \mathbf{W}^{-1} \right) \begin{pmatrix} \alpha \\ 1 \end{pmatrix} \right\| \\ &\leq C \left\| \widetilde{\mathbf{W}}^{-1} - \mathbf{W}^{-1} \right\| \\ &\leq C' \left\| \widetilde{\mathbf{W}} - \mathbf{W} \right\|, \end{aligned} \quad (34)$$

where  $\|.\|$  stands for any standard matrix norm. The last inequality comes from the application of the binomial inverse theorem (see for instance Henderson and Searle 1981 or Chang 2006). Finally, (33) and (34) lead to the following rate of convergence

$$\|\tilde{w}_{T_k} - w_{T_k}\|_\infty = O(h_L^2) + O_P \left( \{n h_L^6\}^{-1/3} \right), \quad (35)$$

and as a by-product of (8), (32), and (35), one gets

$$\left\| \tilde{S}_{T_k} - S_{T_k} \right\|_\infty = O(h_L^2) + O_P \left( \{n h_L^6\}^{-1/3} \right). \quad (36)$$

Both previous rates of convergence are the two first claimed ones in Theorem 2. By using similar arguments, one can derive the asymptotic behaviour of the derivative of the shape profiles and warping functions. To this end, just remark that  $w'_{T_k}(t) = (1, 2t) \mathbf{W}^{-1} \begin{pmatrix} \alpha \\ 1 \end{pmatrix}$  and  $\tilde{w}'_{T_k}(t) = (1, 2t) \widetilde{\mathbf{W}}^{-1} \begin{pmatrix} \alpha \\ 1 \end{pmatrix}$ . In the similar way than the study of  $\tilde{w}_{T_k}(t)$ , it is easy to get the third result of Theorem 2:

$$\|\tilde{w}'_{T_k} - w'_{T_k}\|_\infty = O(h_L^2) + O_P \left( \{n h_L^6\}^{-1/3} \right). \quad (37)$$

About the shape profile, one has

$$S'_{T_k} = (w_{T_k}^{-1})' (L'_{T_k} \circ w_{T_k}^{-1}) \text{ and } \tilde{S}'_{T_k} = (\tilde{w}_{T_k}^{-1})' (\tilde{L}'_{T_k} \circ \tilde{w}_{T_k}^{-1}),$$

and it comes:

$$\begin{aligned} \left| \tilde{S}'_{T_k}(u) - S'_{T_k}(u) \right| &\leq \left| (\tilde{w}_{T_k}^{-1})'(u) \left\{ \tilde{L}'_{T_k} \circ \tilde{w}_{T_k}^{-1}(u) \right\} - (w_{T_k}^{-1})'(u) \left\{ L'_{T_k} \circ w_{T_k}^{-1}(u) \right\} \right| \\ &\leq \underbrace{\left| \tilde{L}'_{T_k} \circ \tilde{w}_{T_k}^{-1}(u) \right|}_{T_1} \underbrace{\left| \tilde{w}_{T_k}^{-1}(u) - w_{T_k}^{-1}(u) \right|}_{T_2} \\ &\quad + \underbrace{\left| \tilde{L}'_{T_k} \circ \tilde{w}_{T_k}^{-1}(u) - L'_{T_k} \circ w_{T_k}^{-1}(u) \right|}_{T_3} \underbrace{\left| w_{T_k}^{-1}(u) \right|}_{T_4}. \end{aligned} \quad (38)$$

- By remarking that  $T_1 \leq \left| \tilde{L}'_{T_k} \circ \tilde{w}_{T_k}^{-1}(u) - L'_{T_k} \circ \tilde{w}_{T_k}^{-1}(u) \right| + \left| L'_{T_k} \circ \tilde{w}_{T_k}^{-1}(u) \right|$ , and according to the smoothness assumption on  $L_{T_k}$  and the asymptotic property of  $\tilde{L}'_{T_k}$ , one has  $\sup_u T_1 < M < \infty$ .
- Thanks to a previous result,  $\sup_u T_2 \leq C \|\tilde{w}_{T_k} - w_{T_k}\|_\infty$ .

- According to the following decomposition

$$T_3 \leq \left| \tilde{L}'_{T_k} \circ \tilde{w}_{T_k}^{-1}(u) - L'_{T_k} \circ \tilde{w}_{T_k}^{-1}(u) \right| + \left| L'_{T_k} \circ \tilde{w}_{T_k}^{-1}(u) - L'_{T_k} \circ w_{T_k}^{-1}(u) \right|,$$

which results in

$$\sup_u T_3 \leq \left\| \tilde{L}'_{T_k} - L'_{T_k} \right\|_{\infty} + \left\| L''_{T_k} \right\|_{\infty} \left\| \tilde{w}_{T_k}^{-1} - w_{T_k}^{-1} \right\|_{\infty},$$

the last term on the right side coming from the taylor expansion of  $L'_{T_k}$ .

As  $T_4 \leq 1$  by construction, the combination of the last results with (9), (35), and (38) leads to the last result of Theorem 2:

$$\left\| \tilde{S}'_{T_k} - S'_{T_k} \right\|_{\infty} = O(h_L^2) + O_P \left\{ (nh_L^6)^{-1/3} \right\}. \quad (39)$$

### B.3 Proof of Theorem 3

It is easy to see that:

$$\left\| \hat{S}_T - S_T \right\|_{\infty} \leq \frac{\sum_{k=1}^K \left\{ \left\| \tilde{S}_{T_k} - S_{T_k} \right\|_{\infty} + \left\| S_{T_k} - S_T \right\|_{\infty} \right\} K_S \left\{ h_S^{-1}(T_k - T) \right\}}{\sum_{k=1}^K K_S \left\{ h_S^{-1}(T_k - T) \right\}},$$

and by combining (36) with the uniform Lipschitz property of the function  $T \mapsto S_T$  (see H2), it comes:

$$\left\| \hat{S}_T - S_T \right\|_{\infty} = O(h_L^2) + O(h_S) + O_P \left( \left\{ nh_L^6 \right\}^{-1/3} \right). \quad (40)$$

Of course, in a similar way one can also estimate the warping function  $w_T$  for any temperature  $T$  from the  $K$ -sample  $(\tilde{w}_{T_1}, T_1), \dots, (\tilde{w}_{T_K}, T_K)$  and one gets:

$$\left\| \hat{w}_T - w_T \right\|_{\infty} = O(h_L^2) + O(h_w) + O_P \left( \left\{ nh_L^6 \right\}^{-1/3} \right). \quad (41)$$

Finally, it is easy to derive an estimation of the constant temperature growth profile  $L_T$  for any temperature  $T$  by recombining the estimated growth shape  $\hat{S}_T$  with the estimated warping function  $\hat{w}_T$ :  $\hat{L}_T := \hat{S}_T \circ \hat{w}_T$ . The consistency of  $\hat{L}_T$  is obtained by decomposing  $\hat{L}_T(t) - L_T(t)$  as follows:

$$\begin{aligned} \left| \hat{L}_T(t) - L_T(t) \right| &\leq \left| \hat{S}_T \circ \hat{w}_T(t) - S_T \circ \hat{w}_T(t) \right| + \left| S_T \circ \hat{w}_T(t) - S_T \circ w_T(t) \right| \\ &\leq \left\| \hat{S}_T - S_T \right\|_{\infty} + \underbrace{\left| S_T \{ \hat{w}_T(t) \} - S_T \{ w_T(t) \} \right|}_A. \end{aligned}$$

So, as soon as you combine (40) and (41) with a taylor expansion of  $S_T$  to process the quantity  $A$ , for any ambient temperature  $T$  it holds:

$$\left\| \hat{L}_T - L_T \right\|_{\infty} = O(h_L^2) + O(h_S) + O_P \left( \left\{ nh_L^6 \right\}^{-1/3} \right), \quad (42)$$

which provides to the first part of Theorem 3. Let us now focus on the estimation of  $S'_T$  and  $w'_T$  at any temperature  $T$ . By using similar arguments, it comes

$$\left\| \hat{S}'_T - S'_T \right\|_{\infty} = O(h_L^2) + O(h_{S'}) + O_P \left\{ (nh_L^6)^{-1/3} \right\}, \quad (43)$$

and

$$\|\widehat{w}'_T - w'_T\|_\infty = O(h_L^2) + O(h_{w'}) + O_P\left(\{nh_L^6\}^{-1/3}\right). \quad (44)$$

Because  $\widehat{L}'_T = (\widehat{S}'_T \circ \widehat{w}_T) \widehat{w}'_T$  and  $L'_T = (S'_T \circ w_T) w'_T$  it comes:

$$\begin{aligned} \|\widehat{L}'_T - L'_T\|_\infty &= \|\widehat{w}'_T (\widehat{S}'_T \circ \widehat{w}_T) - w'_T (S'_T \circ w_T)\|_\infty \\ &\leq (\|\widehat{w}'_T - w'_T\|_\infty + \|w'_T\|_\infty) \underbrace{\|\widehat{S}'_T \circ \widehat{w}_T - S'_T \circ w_T\|_\infty}_A \\ &\quad + \|\widehat{w}'_T - w'_T\|_\infty \|S'_T\|_\infty. \end{aligned} \quad (45)$$

Now, let us focus on  $A$ :

$$\begin{aligned} A &\leq \|\widehat{S}'_T \circ \widehat{w}_T - S'_T \circ \widehat{w}_T\|_\infty + \|S'_T \circ \widehat{w}_T - S'_T \circ w_T\|_\infty \\ &\leq \|\widehat{S}'_T - S'_T\|_\infty + C \|\widehat{w}_T - w_T\|_\infty, \end{aligned} \quad (46)$$

the last quantity of the right side in the previous inequality coming from the Taylor expansion of  $S'_T$ . According to the smoothness of  $w_T$  and  $S_T$ ,  $\|w'_T\|_\infty$  and  $\|S'_T\|_\infty$  are upper bounded and the combination of (41), (43), (44), and (46) results in the second part of Theorem 3:

$$\|\widehat{L}'_T - L'_T\|_\infty = O(h_L^2) + O(h_{S'}) + O(h_w) + O(h_{w'}) + O_P\left((nh_L^6)^{-1/3}\right). \quad (47)$$

#### B.4 Proof of Theorem 4

According to the definition of  $L$  and  $\widehat{L}$ , one can write:

$$\widehat{L}(t_p) - L(t_p) = \sum_{\ell=1}^p (t_{\ell+1} - t_\ell) \left\{ \widehat{L}'_{T(t_\ell)} \circ \widehat{L}_{T(t_\ell)}^{-1} \circ \widehat{L}(t_\ell) - L'_{T(t_\ell)} \circ L_{T(t_\ell)}^{-1} \circ L(t_\ell) \right\} + O(p^{-1})$$

As a by-product, one gets

$$\|\widehat{L} - L\|_\infty \leq C \sup_{\ell} \underbrace{\left\| \widehat{L}'_{T(t_\ell)} \circ \widehat{L}_{T(t_\ell)}^{-1} \circ \widehat{L} - L'_{T(t_\ell)} \circ L_{T(t_\ell)}^{-1} \circ L \right\|_\infty}_{A_{t_\ell}} + O(p^{-1}). \quad (48)$$

Let us now focus on the quantity  $A_{t_\ell}$ :

$$\begin{aligned} A_{t_\ell} &\leq \left\| \widehat{L}'_{T(t_\ell)} \circ \widehat{L}_{T(t_\ell)}^{-1} \circ \widehat{L} - L'_{T(t_\ell)} \circ \widehat{L}_{T(t_\ell)}^{-1} \circ \widehat{L} \right\|_\infty \\ &\quad + \left\| L'_{T(t_\ell)} \circ \widehat{L}_{T(t_\ell)}^{-1} \circ \widehat{L} - L'_{T(t_\ell)} \circ L_{T(t_\ell)}^{-1} \circ L \right\|_\infty \\ &\leq \left\| \widehat{L}'_{T(t_\ell)} - L'_{T(t_\ell)} \right\|_\infty + \left\| L'_{T(t_\ell)} \circ \widehat{L}_{T(t_\ell)}^{-1} \circ \widehat{L} - L'_{T(t_\ell)} \circ L_{T(t_\ell)}^{-1} \circ \widehat{L} \right\|_\infty \\ &\quad + \left\| L'_{T(t_\ell)} \circ L_{T(t_\ell)}^{-1} \circ \widehat{L} - L'_{T(t_\ell)} \circ L_{T(t_\ell)}^{-1} \circ L \right\|_\infty \\ &\leq \left\| \widehat{L}'_{T(t_\ell)} - L'_{T(t_\ell)} \right\|_\infty + \left\| \widehat{L}_{T(t_\ell)}^{-1} - L_{T(t_\ell)}^{-1} \right\|_\infty \|L''_{T(t_\ell)}\|_\infty \\ &\quad + \left\| \widehat{L}_{T(t_\ell)} - L_{T(t_\ell)} \right\|_\infty \|L''_{T(t_\ell)}\|_\infty. \end{aligned} \quad (49)$$

By dividing the domain of  $L_{T(t_\ell)}$  into ranges where  $L_{T(t_\ell)}$  is strictly monotone and involving similar arguments than those used for studying the inverse of the warping function, it holds:

$$\left\| \widehat{L}_{T(t_\ell)}^{-1} - L_{T(t_\ell)}^{-1} \right\|_\infty \leq C \left\| \widehat{L}_{T(t_\ell)} - L_{T(t_\ell)} \right\|_\infty. \quad (50)$$

Now, (42), (47), and (48)-(50) allows us to get:

$$\begin{aligned} \|\widehat{L} - L\|_\infty &= O(h_L^2) + O(h_S) + O(h_{S'}) + O(h_w) \\ &\quad + O(h_{w'}) + O(p^{-1}) + O_P\{(nh_L^6)^{-1/3}\}. \end{aligned} \quad (51)$$

From the dynamic growth model, one can estimate the derivative of  $L$  with  $\widehat{L}'(t) = \widehat{L}'_{T(t)} \circ \widehat{L}_{T(t)}^{-1} \circ \widehat{L}(t)$ . Then, it is easy to see that  $\widehat{L}'(t) - L'(t) = A_t$  where the quantity  $A_t$  has been studied to state the last result. So, by involving the asymptotic behaviour of  $\widehat{L}_{T(t)}$  and  $\widehat{L}'_{T(t)}$ , it comes:

$$\begin{aligned} \|\widehat{L}' - L'\|_\infty &= O(h_L^2) + O(h_S) + O(h_{S'}) + O(h_w) + O(h_{w'}) \\ &\quad + O(p^{-1}) + O_P\{(nh_L^6)^{-1/3}\}. \end{aligned} \quad (52)$$

The ultimate task is to estimate the hatching date  $t_h$  and the post mortem interval  $pmi := t^* - t_h$ . Let  $Q(t) := \{L(t^* - t) - L(t^* - t_h)\}^2$  be the theoretical version of  $\widehat{Q}(t)$ . By using a Taylor expansion of  $Q'$  and because  $\widehat{Q}'(\widehat{t}_h) = 0$  and  $Q'(t_h) = 0$ , it comes that  $Q'(\widehat{t}_h) - \widehat{Q}'(\widehat{t}_h) = (\widehat{t}_h - t_h)Q''(\eta)$  with  $\eta \in (\min\{\widehat{t}_h, t_h\}, \max\{\widehat{t}_h, t_h\})$ . So, as soon as  $Q''$  is nonnull in a neighbourhood of  $t_h$ , one gets  $|\widehat{t}_h - t_h| \leq C\|Q' - \widehat{Q}'\|_\infty$ . According to the definition of  $Q$  and  $\widehat{Q}$ , one can write:

$$\begin{aligned} Q'(\widehat{t}_h) - \widehat{Q}'(\widehat{t}_h) &= 2 \left\{ L'(t^* - \widehat{t}_h) - \widehat{L}'(t^* - \widehat{t}_h) \right\} \{L(t^* - \widehat{t}_h) - L(t^* - t_h)\} \\ &\quad + 2 \left\{ \widehat{L}'(t^* - \widehat{t}_h) - L'(t^* - \widehat{t}_h) \right\} \{ \widehat{L}(t^* - \widehat{t}_h) - L(t^* - \widehat{t}_h) \} \\ &\quad + 2 \left\{ \widehat{L}'(t^* - \widehat{t}_h) - L'(t^* - \widehat{t}_h) \right\} \{ \overline{Y}^* - L(t^* - t_h) \} \\ &\quad + 2 L'(t^* - t_h) \left\{ \widehat{L}(t^* - \widehat{t}_h) - L(t^* - \widehat{t}_h) + \overline{Y}^* - L(t^* - t_h) \right\}. \end{aligned}$$

Because  $\overline{Y}^* - L(t^* - t_h) = O_P(n_{obs}^{-1/2})$ , the asymptotic properties (51)-(52) of  $\widehat{L}$  and  $\widehat{L}'$  the claimed result in Theorem 4 holds:

$$\begin{aligned} \widehat{t}_h - t_h &= O(h_L^2) + O(h_S) + O(h_{S'}) + O(h_w) + O(h_{w'}) \\ &\quad + O(p^{-1}) + O_P\{(nh_L^6)^{-1/3}\} + O_P(n_{obs}^{-1/2}). \end{aligned}$$

As a by-product, one gets the consistency of the post mortem interval:

$$\begin{aligned} \widehat{pmi} - pmi &= O(h_L^2) + O(h_S) + O(h_{S'}) + O(h_w) + O(h_{w'}) \\ &\quad + O(p^{-1}) + O_P\{(nh_L^6)^{-1/3}\} + O_P(n_{obs}^{-1/2}). \end{aligned}$$

## References

J. Amendt, C.P. Campobasso, E. Gaudry, C. Reiter, H.N. LeBlanc, and M.J.R. Hall. Best practice in forensic entomology standards and guidelines. *International journal of legal medicine*, 121(2):90–104, 2007.

P. Bhadra, A.J. Hart, and M.J.R. Hall. Factors affecting accessibility to blowflies of bodies disposed in suitcases. *Forensic science international*, 239:62–72, 2014.

F.C. Chang. Inversion of a perturbed matrix. *Applied mathematics letters*, 19(2):169–173, 2006.

S.E. Donovan, M.J.R. Hall, B.D. Turner, and C.B. Moncrieff. Larval growth rates of the blowfly, *calliphora vicina*, over a range of temperatures. *Medical and veterinary entomology*, 20(1):106–114, 2006.

J. Fan. Design-adaptive nonparametric regression. *Journal of the American statistical Association*, 87(420):998–1004, 1992.

J. Fan. Local linear regression smoothers and their minimax efficiencies. *The Annals of Statistics*, pages 196–216, 1993.

J. Fan and I. Gijbels. Variable bandwidth and local linear regression smoothers. *The Annals of Statistics*, pages 2008–2036, 1992.

F. Ferraty and P. Vieu. *Nonparametric functional data analysis: theory and practice*. Springer Science & Business Media, 2006.

F. Ferraty, A. Laksaci, A. Tadj, and P. Vieu. Kernel regression with functional response. *Electronic Journal of Statistics*, 5:159–171, 2011.

B. Greenberg. Flies as forensic indicators. *Journal of Medical Entomology*, 28(5):565–577, 1991.

H.V. Henderson and S.R. Searle. On deriving the inverse of a sum of matrices. *Siam Review*, 23(1):53–60, 1981.

L. Horváth and P. Kokoszka. *Inference for functional data with applications*, volume 200. Springer Science & Business Media, 2012.

J.S. Marron, J.O. Ramsay, L.M. Sangalli, and A. Srivastava. Statistics of time warpings and phase variations. *Electronic Journal of Statistics*, 8(2):1697–1702, 2014.

D. Martín-Vega, T.J. Simonsen, and M.J.R. Hall. Looking into the puparium: Micro-ct visualization of the internal morphological changes during metamorphosis of the blow fly, *calliphora vicina*, with the first quantitative analysis of organ development in cyclorrhaphous dipterans. *Journal of Morphology*, 2017.

J.O. Ramsay and B.W. Silverman. *Functional Data Analysis*. Springer, 2005.

S. Reibe and B. Madea. How promptly do blowflies colonise fresh carcasses? a study comparing indoor with outdoor locations. *Forensic Science International*, 195(1):52–57, 2010.

C.S. Richards, C.C. Rowlinson, and M.J.R. Hall. First full developmental data set for *calliphora vomitoria* and a consideration for the accumulated degree hour development model. *in preparation*, 2017.

D. Ruppert and M. P. Wand. Multivariate locally weighted least squares regression. *The annals of statistics*, pages 1346–1370, 1994.

J.-A. Warren, T. D. Pulindu Ratnasekera, D. A. Campbell, and G. S. Anderson. Initial investigations of spectral measurements to estimate the time within stages of protophormia terraenovae (robineau-desvoidy) (diptera: Calliphoridae). *Forensic Science International*, 278:205 – 216, 2017. ISSN 0379-0738.